THERAPEUTIC ADVANCES in
Urology

Review

Multiparametric ultrasound of prostate: role in prostate cancer diagnosis

Ther Adv Urol

2022, Vol. 14: 1–24

DOI: 10.1177/17562872221145625

Masatomo Kaneko, Maria Sarah L. Lenon, Lorenzo Storino Ramacciotti, Luis G. Medina, Aref S. Sayegh, Anibal La Riva Rincon, Laura C. Perez, Alireza Ghoreifi, Maria Lizana, Donya S. Jadvar, Amir H. Lebastchi, Giovanni E. Cacciamani and Andre Luis Abreu

***Abstract*:** Recent advances in ultrasonography (US) technology established modalities, such as Doppler-US, HistoScanning, contrast-enhanced ultrasonography (CEUS), elastography, and micro-ultrasound. The early results of these US modalities have been promising, although there are limitations including the need for specialized equipment, inconsistent results, lack of standardizations, and external validation. In this review, we identified studies evaluating multiparametric ultrasonography (mpUS), the combination of multiple US modalities, for prostate cancer (PCa) diagnosis. In the past 5 years, a growing number of studies have shown that use of mpUS resulted in high PCa and clinically significant prostate cancer (CSPCa) detection performance using radical prostatectomy histology as the reference standard. Recent studies have demonstrated the role mpUS in improving detection of CSPCa and guidance for prostate biopsy and therapy. Furthermore, some aspects including lower costs, real-time imaging, applicability for some patients who have contraindication for magnetic resonance imaging (MRI) and availability in the office setting are clear advantages of mpUS. Interobserver agreement of mpUS was overall low; however, this limitation can be improved using standardized and objective evaluation systems such as the machine learning model. Whether mpUS outperforms MRI is unclear. Multicenter randomized controlled trials directly comparing mpUS and multiparametric MRI are warranted.

Keywords: multiparametric ultrasonography, prostate biopsy, prostate cancer

Received: 17 February 2022; revised manuscript accepted: 25 November 2022.

Correspondence to:
Andre Luis Abreu
Center for Image-Guided Surgery, Focal Therapy, and Artificial Intelligence for Prostate Cancer, USC Institute of Urology and Catherine & Joseph Aresty Department of Urology, Keck School of Medicine, University of Southern California, 1441 Eastlake Ave, Suite 7416, Los Angeles, CA 90089, USA

Department of Radiology, Keck School of Medicine, University of Southern California, Los Angeles, CA, USA.
andre.abreu@med.usc.edu

Masatomo Kaneko
Center for Image-Guided Surgery, Focal Therapy, and Artificial Intelligence for Prostate Cancer, USC Institute of Urology, Keck School of Medicine, University of Southern California, Los Angeles, CA, USA

Department of Urology, Graduate School of Medical Science, Kyoto Prefectural University of Medicine, Kyoto, Japan

Maria Sarah L. Lenon
Lorenzo Storino Ramacciotti
Luis G. Medina
Aref S. Sayegh
Anibal La Riva Rincon
Laura C. Perez
Alireza Ghoreifi
Maria Lizana
Amir H. Lebastchi
Center for Image-Guided Surgery, Focal Therapy, and Artificial Intelligence for Prostate Cancer, USC Institute of Urology, Keck School of Medicine, University of Southern California, Los Angeles, CA, USA

Donya S. Jadvar
Dornsife School of Letters and Science, University of Southern California, Los Angeles, CA, USA

Introduction

Prostate cancer (PCa) is the second most frequent cancer and the fifth highest cause of cancer death among males worldwide in 2020.[1] Transrectal ultrasound (TRUS) prostate biopsy (PBx) has been the gold standard for diagnosing PCa.[2] Although TRUS has several strengths including availability, cost-effectiveness, familiarity to urologists, and ability to real-time guidance, TRUS alone cannot reliably detect PCa.[3] Thus, more accurate diagnostic method is needed.

Currently, magnetic resonance imaging (MRI) enables anatomical/functional imaging of the prostate and visualizes the majority of clinically significant prostate cancer (CSPCa).[4–7] Interpretation of multiparametric magnetic resonance imaging (mpMRI) sequences is standardized by the Prostate Imaging Reporting and Data System (PIRADS).[8] Using software to fuse previously obtained mpMRI and real-time TRUS images, the MRI/TRUS fusion PBx integrates the advantages of both MRI, with its ability for lesion detectability, and TRUS, with its real-time imaging guidance.[6,9] MRI-visible lesion can be precisely sampled by MRI/TRUS fusion targeted PBx, and each biopsy trajectory with spatial coordinates in the prostate is recorded in the MRI/TRUS fusion software for review. In fact, MRI/TRUS fusion PBx gained popularity and mpMRI prior to PBx for all men with a suspicion for PCa is recommended by guidelines (i.e. European Association

Giovanni E. Cacciamani
Center for Image-Guided Surgery, Focal Therapy, and Artificial Intelligence for Prostate Cancer, USC Institute of Urology, Keck School of Medicine, University of Southern California, Los Angeles, CA, USA

Department of Radiology, Keck School of Medicine, University of Southern California, Los Angeles, CA, USA

Table 1. Features of US modalities.

Modality	Target aspects	Advantages	Disadvantages
B-mode	Anatomy	Availability	Limited performance for TZ tumors
Doppler-US	Macrovascularity	Availability Potential to detect more aggressive PCa	Limited performance for TZ tumors False positive due to prostatitis
HistoScanning	Software analysis of US radiofrequency data	Automated analysis of tissue heterogeneity, cell density, and vascularity	Dependent to prostate size and operator's experience for motorized TRUS
CEUS	Microvascularity	Ability to show ablated area by FT	Limited performance for TZ tumors Difficulty for scanning the entire prostate Need ultrasound-enhancing agent
Elastography	Stiffness	Cost-effectiveness Availability	Limited performance for PZ tumors False positive due to prostatitis Applying excessive compression may falsely increase tissue stiffness
Micro-US	Anatomy	Three-times higher spatial resolution convenience	Existence of learning curve
mpUS	Combination of the used modalities	Ability to evaluate the integrated aspects of PCa	Difficulty for standardized evaluation Prolonged time

B-mode, brightness-mode; CEUS, contrast-enhanced ultrasonography; FT, focal therapy; mpUS, multiparametric ultrasonography; PCa, prostate cancer; PZ, peripheral zone; TRUS, transrectal ultrasound; TZ, transitional zone; US, ultrasonography.

of Urology, American Urological Association, and Society of Abdominal Radiology). mpMRI, however, has several limitations including availability, the expensive cost, the difficulty for real-time imaging, and low inter-reader agreement.[4,5] In addition, patient/prostate movement, prostate deformation, and the registration error between MRI and TRUS images may have impact on the tumor detection and localization.[10,11]

Recent advances in ultrasonography (US) technology established US modalities, such as Doppler-US, HistoScanning, contrast-enhanced ultrasonography (CEUS), elastography, and micro-ultrasound (micro-US).[12–17] Although these new modalities have some limitations including need of specialized equipment, inconsistent results, lack of standardizations, and external validation, the early results of multiparametric US have been promising (Table 1).[18–23] The 'Multiparametric Ultrasound (mpUS)' is attracting attention in the field of Urology and Radiology. The European Association of Urology (EAU) guidelines on PCa mentioned mpUS as a promising imaging approach for PCa diagnosis, but they also pointed out that lack of standardization and lack of large-scale evaluation were drawback.[24] Currently, it is not stated on guidelines whether mpUS should be a supplemental or standalone imaging technique on PCa diagnosis. Herein, we review studies focusing on the role of new US modalities and mpUS in PCa diagnosis and describe future directions.

Ultrasound modalities in use for PCa diagnosis

Brightness-mode TRUS

Conventional US images are usually generated on the brightness (B) mode.[25] The characterization of tissues in B-mode US images is possible through the evaluation of acoustic parameters such as attenuation and backscattering coefficients

obtained from radiofrequency (RF) echo signals.[26] B-mode US images display maps of echo-signal amplitude on a monitor with gray-scale, pixel-brightness values that are a function of the video signal.[27] First, the probe emits a short US pulse that will penetrate deep into the tissue or, when encountering a tissue with a different acoustic impedance, be reflected toward the transducer. Images are then created by detecting these back-scattered US waves. The length of the ultrasonic waves and the various acoustic impedances impact the generation of a B-mode image.[28,29]

B-mode imaging has limitations in PCa detection as the backscatter signals from PCa, and normal prostate can be similar (Figure 1(a)). There also tends to be heterogeneity in the signals generated from the transition zone in this mode of sonographic imaging.[30] Furthermore, when different settings are utilized to generate B-mode images of the same tissue, such as gain and time-gain compensation settings, diverse images are expected to be visualized. Using the same imaging settings between different operators may help mitigate this the most.[28]

Traditionally, B-mode sonographic imaging has been utilized as a part of the primary detection method of PCa. TRUS B-mode imaging has been extensively studied to assess its diagnostic capacity for detecting PCa. Its advantages include providing real-time images and being the most accessible, economical, and least harmful medical imaging device.[26] The sensitivity and specificity of conventional B-mode TRUS are limited and range from 40 to 50% in PCa detection from most studies, however.[30] According to Postema *et al.*,[29] TRUS Standard B-mode has sensitivity in PCa detection ranging only from 11 to 35% and a positive predictive ranging from 17 to 57%. The utility of B-mode ultrasound, however, has been seemingly undermined according to Steinkohl *et al.*,[31] who showed that the B-mode TRUS imaging of the prostate could detect up to 62% of mpMRI-visible lesions, which is currently the most accurate imaging modality. In addition, B-mode has been regarded as insufficiently accurate for tumor detection, making systematic US-guided biopsies necessary. Systematic biopsy is a widely accepted practice for PCa detection in which samples from pre-defined anatomical zones of the prostate are retrieved in a nontargeted manner.[26] Given the randomness of this approach, however, it causes an increase in false-negative rates up to 35%.[31]

Doppler-US. Color Doppler ultrasonography (CDUS) has been proposed as a tool to improve the accuracy of TRUS using other parameter than echogenicity on regular B-mode US.[12] The vascularity of a suspicious hypoechoic area on regular gray-scale B-mode US can be identified and characterized by CDUS or Power Doppler ultrasonography (PDUS).[32] Although PDUS is more sensitive than CDUS in detecting slow blood flow, PDUS has not shown better PCa detection than CDUS.[32] In addition, PDUS does not depict the direction of the blood flow.[22]

Angiogenesis is one of the pathologic hallmarks for the growth of tumors. A Doppler shift is defined as the wavelength difference caused by the movement of an object. The principle behind Doppler-US is to help identify the wavelength changes reflecting the moving cells within the bloodstream.[33] Therefore, an increased number of shifts is associated with neovascularization in that tissue.[22,17]

The Doppler flow patterns between malignant and benign lesions were assessed by Ashi *et al.*[12] In that series, the median velocity of PCa lesions was 1.35 cm/s compared with a median of 0.36 cm/s for their benign counterparts. In addition to that, the flow was continuous and phasic for malignant lesions *versus* irregular on benign ones. The flow characteristics seen on PCa areas are possibly related to the higher number of vessels, increased diameter, and reduced flow resistance. The lack of smooth muscle on neovascularized vessels explains the reduced resistance to flow. Furthermore, the increased cell volume within the lesion can constrict these vessels, increasing flow velocity. CDUS can detect vessels as small as 1 mm, yet microvessels in prostate malignancies are as little as 10 microns, representing a diagnostic challenge for this tool. Nevertheless, PDUS can be used to increase the sensitivity to smaller vessels (less than 2 mm).[17,34]

When evaluating a PCa lesion with CDUS, different flow patterns have been described: (1) focal within the lesion, (2) flow surrounding the lesion, and (3) diffuse flow within the lesion, the latter being the most common pattern (Figure 1(b)).[32]

Kuligowska *et al.*[35] reported PCa diagnostic performance of CDUS using 544 PBx patients who underwent sextant biopsy and targeted biopsy of US abnormalities. Sensitivity/specificity for PCa detection was 41%/85% for TRUS alone,

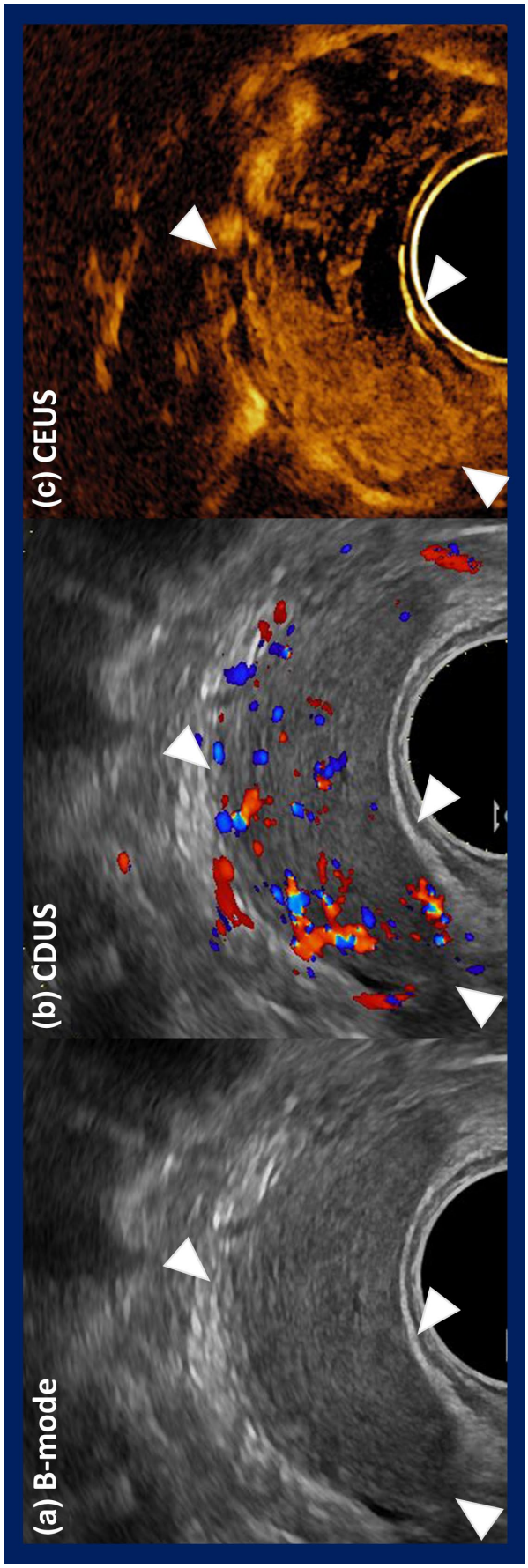

Figure 1. Representative images of B-mode, CDUS, and CEUS. A 55-year-old man with PSA 6.8 ng/ml on active surveillance for GG1 cancer. Follow-up biopsy revealed GG2 cancer on right peripheral zone from apex to base. 2 cm × 1.5 cm hypoechoic lesion (a) with flow surrounding the lesion and diffuse flow within the lesion on CDUS (b) was confirmed (arrowhead). On CEUS imaging, (c) a faster contrast uptake in the right apex of the prostate and regular uptake to the rest of the prostate (arrowhead).
B-mode, brightness-mode; CDUS, color Doppler ultrasonography; CEUS, contrast-enhanced ultrasonography; GG, grade group; PSA, prostate-specific antigen.

43%/66% for CDUS alone, and 57%/61% for the combination. There may be a room for further improving the performance of Doppler-US. Recently, Zeng *et al.*[36] investigated diagnostic performance of three-dimensional (3D) power Doppler ultrasound (3D-PDUS) for CSPCa detection with the virtual organ computer-aided analysis technique. A total of 99 participants with suspicion for PCa prospectively underwent TRUS + PDUS + 3D-PDUS. Using detection of CSPCa on PBx as the reference standard, vascularization index determined by 3D-PDUS achieved 86% of sensitivity and 87% of specificity. The vascularization index was calculated by the percent of color-coded voxels within the volume of interest. CSPCa detection by vascularization index was 82.1% and was statistically higher than TRUS (69.5%) and PDUS (63.4%).

The sensitivity for PCa detection increases when CDUS is utilized, improving diagnostic performance of TRUS. On the contrary, specificity decreases. This can be explained by the fact that prostatitis can be interpreted as a malignant lesion plus the preferential identification of larger and higher-grade lesions with Doppler, in which angiogenesis occurs more frequently.[37,38] Therefore, inflammatory changes or conditions within the prostate can be easily confused with a malignancy without the proper clinical correlation. CDUS can also be used in other situations such as surveillance comparisons on repeat biopsies or as a marker of not viable tissue after local treatments for PCa by measuring the absence of Doppler signals.[38] Major limitations of CDUS are operator-dependency and lack of standardization.

Superb microvascular imaging (SMI) is a novel technology that visualizes slow microvascular blood flow.[33] While conventional Doppler-US may depict clutter signals caused by tissue movement, SMI suppress the clutter to specifically detect blood flow signal owing to its machine algorithm.[39] Compared with conventional Doppler-US, SMI may visualize slow blood flow with high frame rates, high resolution, high sensitivity, and less motion artifact. Zhu *et al.*[33] found SMI detected blood vessels in 97.3% of patients with PCa, and there was a positive correlation between the quantity of microvascular on SMI and biopsy Gleason score. Interestingly, Ohashi *et al.*[40] reported a case in which slow blood flow in the prostate stromal sarcoma (PSS) was detected by SMI. Of note, the intratumoral blood flow was not detected by conventional CDUS. They performed targeted biopsy toward the lesion with the blood flow under SMI-guidance, and viable tumor cells were successfully sampled. They emphasized the usefulness of SMI to target the lesion with intratumoral blood flow indicating viable cells, as PSS often includes a large necrotic area. Furthermore, some researchers performed SMI pre- and post-focal ablation for localized PCa.[39,41] Using SMI, they confirmed presence of tumor blood flow before ablation, and then confirmed disappearance of the blood flow after ablation to define technical success for the ablation.[39,41] Although the impact of SMI on oncological outcomes has not been proven yet, SMI-guided target PBx and focal ablation seems feasible.

HistoScanning. HistoScanning is an ultrasound-based imaging system used to improve accuracy for detection, localization, tumor volume, and suggestive PCa changes, consisting of the scanning and sequentially evaluation of the prostate tissue using a rectal probe.[13] This technology allows a software analysis of unprocessed 3D-reconstructed ultrasound RF data and its comparison with a database preloaded in the system.[13,42] HistoScanning software proposes three different algorithms linked to tissue heterogeneity, cell density, and vascularity to analyze the signals before displaying the results on the screen.[43]

HistoScanning technology is performed in a three-step stepwise manner. First, a TRUS probe connected externally to a motor (motorized TRUS) generates a complete 3D-prostate scan. Second, the operator outlines the regions of interest (ROIs) using the HistoScanning software platform. Finally, a computerized algorithm analysis provides red-coded areas suspicious for PCa and the corresponding tumor volume in a non-real-time manner.[44,45] Yet, in cases in which low-quality imaging data are encountered, purple-coded areas are displayed in the analysis.[44,45]

In a similar fashion to MRI–US fusion modalities, HistoScanning true targeting (HS-TT) allows for the conversion of HistoScanning results to real-time TRUS targets.[13] Following imaging and algorithm analysis, an additional software system provides the operator with commands on how to maneuver the TRUS probe fitted with a needle guide to sample cores from specific, red-coded areas that have been identified.[7,44,45]

In addition, just as the perineal PBx route has gained popularity, the HistoScanning perineal

biopsy route has evolved as well. HistoScanning perineal-guided biopsy is performed with the patient in dorsal lithotomy. The perineal-guided biopsy is performed using a triplane US probe, and the HistoScanning report system, and the brachytherapy template grid as a guide. Therefore, template-guided HistoScanning targeted biopsy can be performed without supplementary procedures.[7]

There has been controversy in the literature regarding HistoScanning performance detecting PCa.[42,46] Some earlier studies show a high HistoScanning accuracy performance characteristic detecting PCa lesions of $\geqslant 0.5\,cm^3$ with sensitivity and specificity up to 100% and 80%, respectively.[47] Despite these early encouraging results, subsequent studies yield controversial findings, with lower sensitivity (37–70.3%) and specificity (14.7–73%).[42,46,48,49] Similarly, a study in which a lower PCa detection lesion $\geqslant 0.1\,cm^3$ reported even lower results (60% and 66%, respectively).[50] Moreover, several studies concluded that HistoScanning accuracy is determined by objective factors such as prostate volume and subjective factors including operator's experience in performing the motorized TRUS that is essential for 3D-reconstructed US RF data.[13] Thus, HistoScanning may represent a valuable tool for experienced operators.

CEUS. Joyner *et al.*,[51] in 1967, described an ultrasonic contrast study while performing an echocardiogram. Instilling saline solution through an intracardiac catheter formed mini bubbles seen as clouds of echoes during the test. CEUS consists of the imaging technique involving the administration of intravenous ultrasound contrast agents to improve the visualization of structures of interest.[52] Specifically, for PCa, this strategy aids in the detection, diagnosis, and follow-up of suspicious lesions while performing targeted PBx with TRUS.

Conventional gray-scale TRUS is limited to detecting PCa or distinguishing ablated prostate from normal prostate with high accuracy. Agents, however, containing microbubbles that improve the visualization of the prostate microvasculature increases the chances for detection of a malignant lesion as prostatic adenocarcinoma is characterized by angiogenesis with increases of microvasculature density (Figure 1(c)).[53] CEUS brings several potential advantages in the management of PCa including diagnosis, facilitating targeted PBx, real-time evaluation and confirmation of adequate tissue ablation after focal therapy (FT), and identification of post-treatment recurrence during post-ablation surveillance by achieving better vascular imaging resolution.[52]

Doppler ultrasound can accurately assess macrovessels but not vessels less than 200 μm as those typically seen with angiogenesis. Ultrasound contrast containing microbubbles measuring 2–6 μm are pure intravascular as they do not cross into the interstitial space, they are small enough to pass through the pulmonary circulation and enter the systemic circulation, but large enough not to escape the endothelium, and excellent to see microvasculature typical of prostate adenocarcinoma.[54,55] The following ultrasound-enhancing agents (UEAs) are approved for use: Lumason® (sulfur hexafluoride lipid-type A microspheres), SonoVue®, Definity®, or Luminity®.[56] UEA do not require laboratory assessments prior to the procedure, and do not have any nephrotoxicity, hepatotoxicity, or cardiotoxicity known. A multi-institutional study of 5576 patients undergoing contrast-enhanced echocardiography reported an adverse event rate of 0.27%, with all adverse events being mild and transient.[57]

CEUS can assess perfusion within the small microvessels (40 μm) seen in PCa with a positive predictive value up to 91.7%, sensitivity up to 79.3%, and accuracy of 83.7%. The addition of CEUS-guided targeted PBx may be associated with significantly improved cancer detection rate compared with 12-core systematic biopsy.[14,58,59,60] Also, it provides immediate intraoperative visualization of ablated area with clear and sharp margins, therefore confirming that the targeted area of suspicious was indeed treated as planned. Of note, CEUS represents a compelling strategy for the evaluation and diagnosis of other urologic malignancies such as kidney and bladder cancer.[61,62]

Proprietary software can process raw data acquired by CEUS.[63] Time-intensity curve (TIC) is depicted by the software plotting echo mean in dB (X-axis) against time (Y-axis). Quantitative parameters such as peak intensity (PI), wash-in slope (WIS), and time-to-peak (TTP) can be acquired from TIC. By comparing TIC extracted from PCa suspicious ROI and contralateral normal ROI, PCa exhibits higher PI, steeper WIS, and earlier TTP.[64,65] Ablated tissue by high-intensity focused ultrasound (HIFU) can be

confirmed as a flat curve with minimal slope on TIC (Figure 2).[52]

Elastography. Ultrasound elastography, an imaging technique that detects and quantifies tissue stiffness, is helpful in diagnosing PCa as malignant tissue has greater stiffness than benign tissue. The two most common types of elastography used on the prostate are strain elastography (SE) and shear-wave elastography (SWE).[66] SE measures the strain seen in the tissue under mechanical stress induced by the transrectal probe. To avoid the risk of applying excessive compression and falsely increasing tissue stiffness, an inflated balloon (with water, for example) may be used to separate the probe and the rectum.[67] SWE measures the propagation of mechanical waves through a tissue, which can be altered by its stiffness.[68]

SE in the prostate has shown improved accuracy over TRUS in detecting PCa. A meta-analysis with 508 patients comparing SE with histopathology following radical prostatectomy (RP) showed a sensitivity of 72% and specificity of 76% for PCa detection.[69] A systematic review including 1840 patients showed an increase of 7–15% in overall PCa detection when targeted biopsy by TRUS elastography was combined with systematic biopsy compared with systematic biopsy alone.[70] Schiffmann *et al.*,[71] however, did not report similar results. Results of the study involving 679 males and 4074 prostate biopsies from 6 different regions of the prostate demonstrated that SE-targeted biopsy had an overall high value of specificity (90%) and negative predictive value (NPV, 87%) and a low value of sensitivity (19%) and positive predictive value (PPV, 25%). Low sensitivity and PPV suggest that SE may not identify sextants that indeed present PCa.

A systematic review including 2227 patients from 16 SWE studies shows promising results.[72] In nine studies analyzed, systematic biopsy was the reference standard at the per-sample level (core, sextant level). Pooled sensitivity and specificity were 85% and 85%, respectively. When histopathology of RP was used as the reference standard, pooled sensitivity and specificity were 71% and 74%, respectively. Fu *et al.*[73] also demonstrated positive results in their prospective study of 221 patients that compared SWE with MRI of the prostate. Sensitivity, specificity, PPV, NPV, and accuracy were 78.97%, 90.67%, 71.30%, 93.66%, and 88.03%, respectively. Between SWE and MRI, there was no statistically significant difference in PCa diagnosis ($p = 0.259$). SWE's diagnostic ability, however, was marginally superior to MRI for CSPCa ($p = 0.013$). Different results were reported by Xiang *et al.*[74] SWE alone was shown to have a lower diagnostic value than MRI alone, but the combination of both imaging modalities demonstrated higher sensitivity than any of the methods alone.

Despite having favorable outcomes, elastography is not without its limitations. First, the manual compression of the prostate by the SE operator may change the tissue's elasticity, limiting the accuracy of the diagnosis.[75,76] This reduces results' reproducibility, as it is dependent on the examiner's skill and experience. Also, there is no method to compress the prostate uniformly. Second, stiff lesions do not necessarily indicate cancer, and cancerous lesions are not always stiff.[77] Confounding factors such as increased prostate volume, calcifications, and fibrous tissue may produce false-positive results. Finally, considerable limitations include the small box, slow frame rates, and penetration issues of SWE.[66]

Elastography of the prostate can be considered as an additional method to detect PCa and guide biopsy. TRUS-targeted biopsy using elastography seems promising, but prospective multicenter studies should be performed to confirm its usefulness. Technique standardization and validation to allow further studies comparison are needed.

Micro-US. Conventional B-mode TRUS performed at 8–12 MHz allows for adequate penetration depth for the prostate; however, the spatial resolution may not be enough to differentiate physiological glandular ducts, acini of the prostate, and malignancies.[78–80] To improve the limited resolution of conventional TRUS, micro-US utilizing 29 MHz transducer has been developed.[78,81] Compared with the conventional TRUS, this higher frequency system can visualize the prostate with three times higher spatial resolution (70 μm).[17] A trade-off, however, exists between the spatial resolution and the penetration depth, because attenuation is proportional to frequency.[82] Thus, the penetration depth of mpUS system is reduced to 50 mm, which still covers the entire prostate in the standard size.[81,83] Current micro-US system only provides sagittal plane that is optimum view for transperineal PBx. The lack of axial images, however, makes MRI-guided software fusion PBx unachievable, although

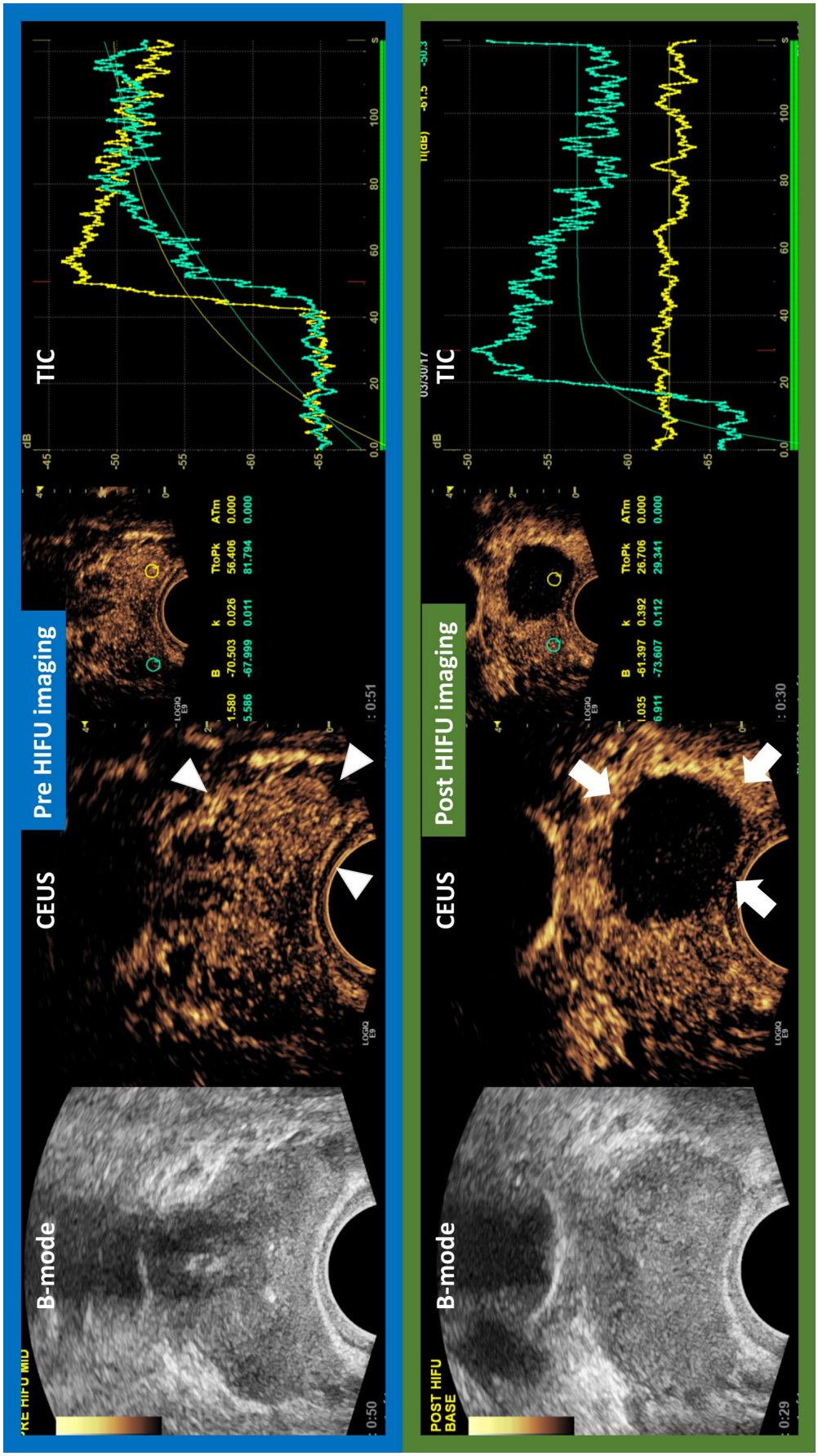

Figure 2. Representative images of pre-/post-HIFU imaging with CEUS. A 62-year-old man with PSA 8.2 ng/ml. Prebiopsy multiparametric MRI revealed PCa suspicious lesion on left side peripheral zone from the base to apex gland level (PIRADS score 5). Systematic 12-core biopsy plus 6-targeted core biopsy revealed GG2 cancer from the left side of the prostate. The patient wished to undergo left hemi-HIFU as a definitive treatment for PCa. Prior to HIFU, CEUS was performed to evaluate vascularity of the bilateral prostate lobes (arrowhead shows contrast enhancement on cancerous area). Time-intensity curves analysis showed higher peak intensity, steeper wash-in slope, and earlier time-to-peak on the left side (yellow circle and yellow graph) of the prostate than those on right side (green circle and green graph). Immediately after HIFU, a second CEUS evaluation was performed to confirm the ablated area (arrow). While the treated side lobe successfully lost vascularity, the contralateral side maintained vascularity. At this point, the procedure was terminated. Postoperatively, PSA dropped to 0.26 ng/ml, follow-up imaging (mpMRI, B-mode TRUS, CDUS, and CEUS) did not detect PCa recurrent suspicious lesion. One year after HIFU, follow-up systematic biopsy confirmed no cancer on both treated and untreated side of the prostate.
B-mode, brightness-mode; CDUS, color Doppler ultrasonography; CEUS, contrast-enhanced ultrasonography; GG, grade group; HIFU, high-intensity focused ultrasound; mpMRI, multiparametric magnetic resonance imaging; PCa, prostate cancer; PIRADS, Prostate Imaging Reporting and Data System; PSA, prostate-specific antigen; MRI, magnetic resonance imaging; TIC, time-intensity curve; TRUS, transrectal ultrasound.

MRI-guided cognitive fusion PBx still can be performed.[84]

Using ultrasonographic appearance of PCa areas on micro-US, a 5-point scoring system for suspicious lesions was created, allowing for more consistent interpretation of prostate images.[81] This grading system is called PRI-MUS (Prostate Risk Identification using Micro-Ultrasound), which is analogous to the PIRADS grading for mpMRI. PRI-MUS 1 and 2 are likely benign. PRI-MUS 3 is associated with intermediate risk of cancer and could be supported by targeted or systematic biopsy. PRI-MUS 4 and 5 lesions are highly correlated to significant disease, and targeted biopsy is indicated.[81,85] Using this grading system, a multi-institutional randomized controlled trial comparing first-generation micro-US with conventional ultrasound-guided PBx was conducted by Pavlovich *et al.*[86] Systematic 12-core transrectal PBx results were used as the reference standard. The trial was split into pre- and post-image interpretation training. The PRI-MUS was developed by the data from the pretraining group, and then used by the post-training group. Improved per-core sensitivity of micro-US in the post-training group compared with the pretraining group was confirmed (60.8% *versus* 24.6%, $p<0.01$), and the sensitivity was significantly higher than conventional TRUS (*versus* 38.0%, $p<0.001$). Moreover, per-patient detection of CSPCa in the micro-US arm improved by 7% after training (32–39%, $p<0.03$). The per-patient CSPCa detection of micro-US, however, was not better than conventional TRUS (34.6% *versus* 36.6 for the entire cohort, and 39.0% *versus* 39.0% for the post-training cohort).

As the first pilot study on the accuracy of micro-US was reported,[78] several studies have compared micro-US with conventional B-mode TRUS and mpMRI.[16,85–88] Zhang *et al.*[89] conducted a meta-analysis of seven studies including 769 patients to analyze the accuracy of micro-US for PBx. They revealed that micro-US had a pooled sensitivity, specificity, diagnostic odds ratio, and area under the summary receiver operating characteristic (ROC) curve of 0.91, 0.49, 10, and 0.82, respectively. Sountoulides *et al.*[90] compared the PCa detection rate of micro-US *versus* mpMRI targeted PBx (TBx) in his meta-analysis of 13 studies containing 1,125 patients. The detection ratio (DR) was estimated as the micro-US TBx detection rate divided by the mpMRI-TBx detection rate. The pooled DR for grade group (GG) 1, ⩾1, ⩾2, and ⩾3 PCa were 0.94, 0.99, 1.05, and 1.25, respectively. Therefore, Sountoulides *et al.*[90] concluded micro-US and mpMRI-TBx showed similar detection rates across all PCa grades. Furthermore, another meta-analysis of 15 studies including 2967 patients by Dariane *et al.*[91] evaluated the added value of micro-US-guided PBx compared with systematic biopsies (SBx). They found micro-US TBx identified more CSPCa [DR = 1.18, 95% confidence interval (CI) = 0.83–1.68] and significantly less GG1 PCa (DR = 0.55, 95% CI = 0.41–0.73) than SBx. The first multicenter prospective study, including 1040 patients, compared diagnostic performance of micro-US with those of mpMRI. Micro-US TBx and mpMRI TBx were taken from PRI-MUS >3 and PIRADS >3 lesion. In the comparison with mpMRI TBx, micro-US TBx showed significantly higher sensitivity (94% *versus* 90%, $p=0.03$) and NPV (85% *versus* 77%, $p=0.04$) with similar specificity (22% *versus* 22%, $p=0.45$) and PPV (44% *versus* 43%, $p=0.32$) for the detection of CSPCa.[92] The results of the OPTIMUM (Optimization of prostate biopsy–Micro-Ultrasound *versus* MRI) study, an ongoing three-arm randomized controlled trial, will determine whether micro-US can be used as an alternative to MRI/TRUS fusion biopsy.[93]

Multiparametric US

As shown above, new US modalities have demonstrated promising results. It, however, is unclear whether one new US modality alone can achieve satisfactory diagnostic performance for PCa. These modalities visualize different aspects of the prostate. The concept of mpUS is similar to mpMRI. Therefore, mpUS is useful for lesion volumetry, guidance for PBx and FT as well. As dynamic contrast imaging on MRI can do, Doppler and CEUS can detect vascularity in PCa tissues. Elastography depicts the stiffness of the prostatic tissue, which may correspond to cancerous cell density. Considering the success of mpMRI for PCa diagnosis, the combination of multiple US modalities also has potential to achieve more reliable performance. Considering several US modalities showing feasibility of guidance for PBx and FT, mpUS may be useful for guidance for PBx and FT as well.[13,39–41,52]

A few groups studied mpUS defined as the combination of 3 or more US modalities.[18–23] In the past 5 years, however, mpUS has gain popularity in urology and radiology field.[30,94–101]

Zhang *et al.*[94] evaluated malignant features of US modalities using 12-core systematic PBx in 40 patients with benign histology and 38 men with a localized PCa as the reference standard. They demonstrate that when US modalities are combined ('⩾3 malignant features' on TRUS or 'asymmetric distribution' on SWE or 'nonsynchronous wash-in/out, unequal enhancement, and heterogeneous distribution' on CEUS), the mpUS achieves high PCa detection performance [sensitivity: 97.4%, specificity: 77.5%, PPV: 80.4%, NPV 96.9%, accuracy: 87.2%, area under the receiver operating characteristic curve (AUROC): 0.874] which was compatible with mpMRI (sensitivity: 94.7%, specificity: 60.0%, PPV: 69.2%, NPV 92.3%, accuracy: 76.9%, AUROC: 0.774). Targeted biopsy, however, was not performed, and therefore, the performance of per lesion was not evaluated. SWE or CEUS is usually evaluated in conjunction with B-mode findings. As the performance of SWE or CEUS (AUROC: 0.860 and 0.859) were similar to mpUS (AUROC: 0.874), the added value of third US modality seems to be limited.

Mannaerts *et al.*[95] prospectively evaluated the CSPCa diagnostic performance of combination of three US modalities (B-mode, SWE, and CEUS) in 48 men undergoing RP as the reference standard. Uniquely, they used an automated RP histopathological correlation method to precisely evaluate CSPCa lesion localization. US modalities were evaluated by three readers using a 5-point Likert-type scale to score 12 anatomical ROI. When Likert-type scale ⩾3 was used as threshold, ROI-specific sensitivity, specificity, PPV, and NPV for CSPCa diagnosis using mpUS were 74%, 59%, 65%, and 70%, respectively. The sensitivity was significantly higher than all single US modalities alone (B-mode: 55%, SWE: 55%, and CEUS: 59%). On the other hand, the specificity was not significantly different from all single US modalities alone (B-mode: 61%, SWE: 61%, and CEUS: 63%). In their subgroup analysis for mpUS performance, ROI-specific sensitivity for the lesion on peripheral zone (PZ) was higher than that on transitional zone (TZ) (80% *versus* 67%). While the sensitivity of SWE alone for PZ tumor was less than B-mode or CEUS alone, B-mode or CEUS alone detects less TZ tumors than SWE. These findings may justify the concept of mpUS as combination of these US modalities. Index lesion (defined as the highest Gleason grade lesion on RP histology) detection rate of ROI1 and ROI2 were significantly higher with mpUS than all single US modalities (mpUS: 88% *versus* CEUS: 73%, B-mode: 72%, or SWE: 70%). Interobserver agreements that were evaluated by the Krippendorff α were not high [mpUS (cut-off value Likert-type ⩾3): 0.33 and mpUS (cut-off value Likert-type ⩾4): 0.48]. Unfortunately, comparison with mpMRI findings was not performed in this study, and the sample size was small. Of note, all participants had PCa that was eventually treated by RP; therefore, population bias likely existed. Compared with single US modalities, mpUS detected more CSPCa on both PZ and TZ. This is a clear advantage of mpUS.

Postema *et al.*[96] evaluated the CSPCa (any GG ⩾3 and GG 2 larger than 0.5 ml) diagnostic performance of B-mode, CEUS, contrast ultrasound dispersion imaging (CUDI), and mpUS (combination of these three US modalities) with 133 men undergoing RP as the reference standard. CUDI, a computer-aided quantification technique, was generated from the CEUS recordings. Likelihood of presenting CSPCa for each imaging modality (B-mode, CEUS, and CUDI) was scored on a 1–5 Likert-type scale by five observers. In their multicenter study, sensitivity/specificity/AUROC for CSPCa diagnosis was 81%/64%/0.78 for CEUS, 83%/55%/0.79 for CUDI, and 83%/55%/0.78 for mpUS. Using a weighted Fleiss Kappa statistic, poor interobserver agreement of US modalities was shown in the study (CEUS: 0.20, CUDI: 0.18, combination: 0.18).

More recently, Grey *et al.*[102] conducted a multicenter prospective paired-cohort study to compare diagnostic performance for CSPCa (any area with GG ⩾3 or maximum cancer core length ⩾6 mm) between mpUS (B-mode + CDUS + elastography + CEUS) *versus* mpMRI. mpMRI evaluation was based on Likert-type system instead of PIRADS, and each US imaging was evaluated with standardized Likert-type scoring method. The overall lesion score was determined at the discretion of the reporter. Using three-core mpUS or mpMRI-targeted PBx as the reference standard, they found CSPCa detection by mpUS alone, mpMRI alone, and the combination of mpUS and mpMRI were 26%, 30%, and 32%, respectively. As a result, 7% of CSPCa were exclusively detected by mpUS alone, whereas 20% of CSPCa were exclusively detected by mpMRI alone. The authors concluded mpUS

could be an alternative to mpMRI as a diagnostic test for patients with high risk of PCa particularly in the case of that mpMRI cannot be performed.

This inconsistent performance and limited interobserver agreement of mpUS may be due to the lack of well-structured or standardized evaluation system. Wildeboer *et al.*[97] assessed the performance of US radiomic features that extracted from B-mode, SWE, and CEUS for the localization of PCa using machine learning methods (a random forest classification algorithm) in their analysis of 48 men with biopsy-confirmed PCa. The RP specimens of these 48 patients were used as the reference standard. While the best-performing single radiomic feature such as contrast velocity achieved a region-wise AUROC of 0.69 for any PCa and 0.76 for CSPCa (defined as PCa > GG2), respectively, multiparametric combination of radiomic features achieved outperforming AUROC of 0.75 for any PCa and 0.90 for CSPCa, respectively. The radiomic features of perfusion-, dispersion-, and elasticity-related features were most frequently selected as effective parameters for PCa classification by machine learning model. Importantly, they also showed that effective radiomic parameters derived from B-mode, SWE, and CEUS were not correlated with each other; therefore, these three modalities may be cumulative. As the selected radiomic parameters substantially differed between the PZ and TZ, they emphasized the necessity for accurate zonal segmentation for US evaluation.

Morris *et al.*[98] evaluated the feasibility of using B-mode, acoustic radiation force impulse imaging (ARFI), SWE, and quantitative ultrasound (QUS) midband fit (MF) to provide image guidance for targeted PBx. ARFI is a US modality to assess elasticity using acoustic radiation force. While SWE provides quantitative stiffness of tissue, ARFI reflects a relative stiffness of tissue. Computing normalized spectra, spectral-based QUS methods quantify the scattering properties of tissues. MF is a most common parameter in QUS analysis which is generated using a linear fit to the normalized backscattered spectra. They acquired B-mode, ARFI, SWE, and MF from 35 men with biopsy-confirmed PCa, and combined them with a linear support vector machine (SVM) method. The SVM was trained and validated by a subset of data from 20 patients and tested by a remaining 15 patients' data. All participants underwent prostatectomy after imaging, whole mount prostates were histologically analyzed and PCa lesions were assigned on a 27-region model as the reference standard. They evaluated contrast and contrast-to-noise ratio (CNR) as lesion visibility metrics and generalized contrast-to-noise ratio (gCNR) as a metric to assess the overlap in the distributions of the two ROIs. mpUS statistically significantly outperformed B-mode and SWE with respect to contrast, CNR, and gCNR, MF with respect to contrast and CNR, and ARFI with respect to CNR. They pointed out that both calcifications and the distance from US probe limited the performance of mpUS.

Future directions

Currently, accurate diagnosis and appropriate stratification of PCa is essential for patient-specific PCa management.[103] Recent advances in PCa imaging technology including mpMRI enabled more precise PCa localization. Whether these new imaging modalities improve clinical outcomes such as overall survival has not been determined yet.[101] Precise imaging, if well validated, may reduce unnecessary PBx and the risk for overdiagnosis and overtreatment.[104] FT based on accurate real-time imaging is expected to achieve better oncological/functional outcomes.[52] Therefore, establishing more precise imaging is important.

Overview of the most up-to-date literature focusing on US for PCa diagnosis is shown on Table 2. Although sample size of the recent studies on mpUS was still small and most of studies were single center, aggregated effectiveness of multiple US modalities likely exists when particular modalities were combined (i.e. B-mode + SWE + CEUS).[94,95,97,98,102] Variation of the combined US modalities are limited so far. Inclusion of state-of-the-art US modality such as SMI or micro-US may further improve the performance of mpUS.

Whether mpUS even outperform mpMRI is unclear, because a few studies directly compared these methods so far.[94,99,102] Multicenter and randomized controlled trials to compare them with large sample size are still needed. Some aspects including lower cost, real-time imaging, applicability for some patients (i.e. claustrophobia or hip prosthesis) who cannot undergo mpMRI, and availability in the office setting are clear advantage of mpUS, compared with mpMRI, however.

Table 2. Overview of the most up-to-date literature on the finding.

First author, year	Study design	Imaging modality	Number of patients	Reference standard	Main findings	Limitations
Lorusso, 2022[105]	Retrospective single-center study	B-mode	64	RP histology	• Sensitivity, specificity, and accuracy for CSPCa detection by ANNA/C-TRUS analysis were 69%, 77%, and 75%, respectively.	• Single-center retrospective study design with small sample size. • RP histology as the reference standard potentially leads to selection bias.
Steinkohl, 2018[31]	Retrospective single-center study	B-mode	142	MRI/TRUS fusion-targeted biopsy	• 92 from 148 mpMRI lesions (62.2%) were visible on B-mode. • Significant influence on the visibility on B-mode: prostate volume (small prostates more visible). • No significant influence on visibility on B-mode: location of the lesion, PIRADS score, size of the lesion.	• Only patients with well-documented MRI/TRUS fusion-targeted biopsy were retrospectively included. • The results were based on an experienced operator equipped by a high-end ultrasound machine.
Garcia-Reyes, 2018[106]	Retrospective single-center study	B-mode	178	MRI/TRUS fusion biopsy (14-core SBx + 2- to 4-core TBx)	• Per location analysis consists of 1331 sextants. • CSPCa detection rate were 20.5% by B-mode alone and 19.7% by mpMRI alone. • The combination of B-mode and MRI showed significantly higher AUC for CSPCa detection (0.85) than B-mode alone (0.80, $p=0.001$) or MRI alone (0.83, $p=0.04$). • The sensitivity and the specificity of B-mode were 42.3% and 91.6%. • The sensitivity and the specificity of MRI were 62.2% and 84.1%.	• Only patients with at least one visible lesion on MRI were retrospectively included.
Zeng, 2022[36]	Prospective single-center study	3D-PDUS	99	TRUS PBx (12-core SBx + 1- to 2-core TBx per lesion)	• Area under the curve for CSPCa detection by the vascularization index and vascularization/flow index was 95% and 95%. • Sensitivity for the vascularization index and vascularization/flow index was 86% and 94%. • Specificity for the vascularization index and vascularization/flow index was 87% and 76%.	• Single technician assessing Doppler. • Lack of comparison with a whole-gland histology.
Ashi, 2021[12]	Prospective single-center study	CDUS	16	TRUS PBx 12–16 cores	• Median microvascular flow velocity of the malignant lesions was 1.25 cm/s compared with 0.36 cm/s for the benign lesions ($p<0.01$). • Median pulsatility index of the malignant lesions was 1.55 *versus* 6.38 for the benign lesions ($p<0.01$). • Median resistive index of the malignant lesions was 0.68 *versus* 1.0 for the benign lesions ($p<0.01$).	• Small sample size.
Zhu, 2019[33]	Prospective single-center study	CDUS and SMI	119	TRUS PBx (10-core SBx + 2- to 3-core SMI-guided TBx)	• SMI and CDUS detected blood vessels of PCa lesion in 97.3% *versus* 90.5%, respectively. • Higher vascular quantity evaluated by SMI and CDUS were significantly correlated to higher Gleason score (correlation coefficient of 0.373 *versus* 0.286). • SMI-guided TBx cores detected significantly more PCa than SBx cores (28.3% *versus* 6.4%, $p<0.001$).	• Only patients with at least one visible lesion on SMI were included. • SMI targets were designated by one SMI expert.
Sarica, 2019[37]	Retrospective single-center study	CDUS	78	TRUS Bx	• The combination of B-mode, CDUS, and PSAD showed highest specificity of PCa detection (80%) compared with each single modality. • The sensitivity, positive, and negative predictive value of the combination were 64%, 64%, and 80%, respectively.	• Subjective grading of vascularity. • No separated CDU imaging record for each biopsy site.

(Continued)

Table 2. (Continued)

First author, year	Study design	Imaging modality	Number of patients	Reference standard	Main findings	Limitations
Vezelis Alvydas, 2020[49]	Prospective single-center study	HistoScanning	200	20-core TTPM PBx	• Sensitivity, specificity, and AUC for CSPCa (GG ⩾3 or an MCCL ⩾6 mm in one location or a TCCL ⩾10 mm in all locations) detection by PHS were 61.9%, 27.85%, and 0.39. • No statistical difference of PHS performance between the groups with prostate under 60 cm^3 and over 60 cm^3.	• No blind trial.
Glybochko, 2019[13]	Prospective single-center study	HistoScanning	611	TRUS PBx (12-core SBx + 1 HistoScanning TBx per lesion)	• When PHS showed PCa suspicion, PCa detection rates per patient were 87% for PHS-TT *versus* 59% for SBx ($p < 0.001$). • When PHS showed PCa suspicion, PCa detection per lesion was 68% for PHS-TT *versus* 25% for SBx ($p < 0.001$). • When PHS showed PCa suspicion, the detection of Gleason group six per patient by PHS-TT was significantly lower than SBx (23.4% *versus* 32.4%, $p = 0.002$).	• Operator-dependent choice of PHS-TT location. • No blind trial. • No STARD-compliant.
Simmons, 2018[46]	Prospective single-center trial	HistoScanning	330	TTPM	• Sensitivity, specificity, and AUC for CSPCa (MCCL ⩾6 mm and Gleason score ⩾4 + 3) by detection by PHS were 70.3%, 14.7%, and 0.43, respectively. • Gland size and lesion volume evaluated between two time points using the same probe were not stable. • Poor accuracy in men requiring further biopsies.	• Only men with clinical suspicion of missed PCa or incorrect classification after TRUS PBx were recruited. • Technical failures with the PHS device and consequent loss of data for reporting. • Real-time targeting technique was not available.
Sharen and Zhang, 2022[107]	Retrospective single-center study	CEUS	46	6-core SBx + 2- to 4-core TBx	• Sensitivity, specificity, and accuracy for PCa detection were 66.7%, 60%, and 65.2% for CEUS, and 84.2%, 81.3%, and 83.3% for SWE, respectively.	• Retrospective study design with small sample size. • Suboptimal reference standard. • The difference in number of cores taken between CEUS and SWE was statistically significant.
Baur, 2018[108]	Prospective single-center study	CEUS	92	2-core MRI/US fusion TBx	• Time to peak measured during CEUS showed significant differences between benign lesion and PCa in peripheral zone (AUC 0.65, sensitivity 69% and specificity 63.3% at optimal cut-off value).	• All patients had at least one previous negative PBx history. • Suboptimal reference standard.
Wildeboer, 2017[14]	Retrospective study	CEUS	19	RP histology	• Sensitivity, specificity, and accuracy for malignant pixels were 79%, 80%, and 81% for the combination of four different parameters related to perfusion and dispersion.	• Retrospective study design with small sample size. • RP histology as the reference standard potentially leads to selection bias.
Eldred-Evans, 2021[109]	Prospective population-based screening study	Elastography (SWE)	403	12-core SBx + B-mode/SWE TBx + MRI/US TBx	• Compared with PSA screening (⩾3 ng/ml), B-mode + SWE did not show the better screening performance than PSA screening alone.	• Participants without any positive screening results did not undergo biopsies.
Liang, 2021[110]	Single-center retrospective study	Elastography (SWE)	112	12-core SBx + 1–2 B-mode/SWE TBx	• The AUCs of radiomic features from B-mode, SWE, and the combination of B-mode and SWE were 0.74, 0.80, and 0.85 for PCa detection, respectively. • Sensitivity and specificity of the combination of B-mode and SWE radiomic features were 77% and 80%, respectively. • When the radiomics model was combined with clinical model (age and PSAD as parameters), the AUC increased to 0.90.	• The impact of zonal difference (PZ *versus* TZ) was not considered for SWE evaluation. • Suboptimal reference standard.

(Continued)

Table 2. (Continued)

First author, year	Study design	Imaging modality	Number of patients	Reference standard	Main findings	Limitations
Fu, 2020[73]	Single-center prospective study	Elastography (SWE)	221	12-core SBx + TRUS or SWE or MRI/US-guided TBx	• Sensitivity and specificity determined by maximum Youden's index for CSPCa (GG ⩾2 and % of cancer in biopsy >50%) detection were 66.2% and 96.1%, respectively. • For CSPCa detection, the AUC of SWE was significantly higher than MRI (0.868 *versus* 0.780, $p=0.013$).	• Transitional zone and central zone were not included. • Suboptimal reference standard.
Ji, 2019[111]	Single-center prospective study	Elastography (SWE)	215	12-core SBx + TRUS TBx	• Young's modulus of elasticity (Emax, Emean, and Emin) was significantly higher in malignant lesion than benign lesion. • Emax, Emean, and Emin sensitivities were 77.88%, 81.42%, and 60.18%, respectively, and the specificities were 85.33%, 74.51%, and 63.73%, respectively. • The GS and PSA both demonstrated a positive correlation with Emax and Emean.	• The prostate gland's stiffness was probably underestimated by the method. • Suboptimal reference standard.
Xiang, 2019[74]	Single-center retrospective study	Elastography (SWE)	356	8–20 core TRUS-Bx	• Sensitivity, specificity, and AUC was 78.3%, 62.4%, and 0.7, respectively, for clinically significant PCa. • SWE alone has a lower diagnostic value than MRI alone.	• Clinically significant PCa from the central zone was not analyzed as SWE was only done at the peripheral zone. • Different equipment was used for the biopsy and SWE assessment.
Ding, 2019[112]	Single-center retrospective study	Elastography	125	12-core SBx + Elastography TBx	• When the Elastographic Q-analysis score cut-off point was 1.95 for differentiating malignant and benign prostate lesions, sensitivity, specificity, and AUC were 83.5%, 84.4%, and 0.87, respectively.	• Large proportion of bilateral or diffuse PCa lesions. • No internal/external validation. • For the goal of achieving a good Elastographic Q-analysis score curve, the operator must be properly trained.
Lughezzani, 2021[113]	Single-center prospective study	Micro-US	320	6–8⩽ core SBx + 2⩽ core per lesion MRI/US fusion TBx + 1⩽ core per lesion micro-US TBx	• The sensitivity and specificity of micro-US for CSPCa detection per patient were 89.7% and 26.0%, respectively. • 2.6% CSPCa cases were detected on micro-US TBx only, whereas 2.6% of CSPCa cases were detected on mpMRI TBx only. • An increasing PRI-MUS score was an independent predictor of CSPCa.	• Observer bias given that all patients had suspicious lesion on MRI (PIRADS ⩾3). • The number of randomized and targeted biopsy cores was not standardized. • An ideal reference standard such as transperineal template mapping biopsies was not used.
Wiemer, 2021[88]	Single-center prospective study	Micro-US	159	mpMRI targeted (2–3 cores) and nontargeted (8–9⩾ cores) biopsies	• The sensitivity and specificity of micro-US for CSPCa detection were 95% and 15%, respectively. • Micro-US TBx detected higher GG than the nontargeted biopsies in 26%, compared with both nontargeted and MRI-targeted biopsies (16%). Micro-US targeting led to 9.4% more upgrade of GG than mpMRI targeting ($p=0.005$).	• All participants had mpMRI positive lesion. • Bias due to a learning curve effect. • Higher number of targets and an increased cancer detection due to including all patients with the indication for a prostate biopsy, even those on active surveillance.
Chessa, 2021[114]	Single-center prospective study	Micro-US	68	3–5 core mpMRI-targeted fusion biopsy	• Sensitivity, specificity, and AUC of micro-US in detection of CSPCa were 68%, 73%, and 0.71 respectively. • Sensitivity, specificity, and AUC of micro-US in detection of CSPCa located in the peripheral zone were 74%, 75%, and 0.75, respectively.	• Only patients with PCa diagnosed by MRI fusion PBx were included. • Lack of experience with micro-US devices and PRI-MUS protocol. • Suboptimal reference standard.

(Continued)

Table 2. (Continued)

First author, year	Study design	Imaging modality	Number of patients	Reference standard	Main findings	Limitations
Avolio, 2021[115]	Single-center retrospective study	Micro-US	111	MRI/US fusion-targeted biopsy	• Sensitivity and specificity of micro-US in detection of CSPCa were 100% and 33.7%, respectively. • PRI-MUS score ⩾3 was an independent predictor of CSPCa (OR = 4.22, $p = 0.001$). • Micro-US was potentially capable to stratify the presence of PCa in patients with an equivocal MRI.	• Operational selection bias as all patients had at least one PIRADS3 lesion. • Suboptimal reference standard.
Klotz, 2020[92]	Prospective multicenter study	Micro-US	1040	TRUS PBx (12- to 14-core SBx and 2- to 3-core from mpMRI and micro-US TBx)	• Micro-US had comparable or higher sensitivity (94% *versus* 90%, $p = 0.03$) for CSPCa compared with mpMRI, with similar specificity (22% *versus* 22% $p = 0.45$).	• Learning curves variability among centers. • Substantial methodological variation existed between sites. • Seven of the 11 sites were unblinded to the MRI when US evaluation was performed.
Claros, 2020[84]	Single-center retrospective study	Micro-US	47	12-core SBx + 3-core TBx	• In targeted biopsies, micro-US cases presented higher detection of CSPCa than robotic MRI/US fusion PBx (38% *versus* 23%, $p = 0.02$). • CSPCa would be missed in 2% of patients in the micro-US group and 9% in the robotic MRI/US fusion PBx group.	• Retrospective nature and lack of randomization. • Only patients with suspicion of PCa on mpMRI were included. • Suboptimal reference standard.
Rodriguez Socarrás, 2020[116]	Single-center retrospective study	Micro-US	194	Ginsburg SBx + 5 core micro-US TBx + 5 core MRI/US fusion TBx (if PIRADS ⩾3)	• Micro-US found 12/108 (11%) prostate cancers that were missed by all other techniques, of which 11 (92%) were CSPCa. • Sensitivity, specificity, PPV, and NPV of micro-US TBx to detect CSPCa per patient were uniformly higher than mpMRI (99.7%, 23.1%, 46.0%, and 99.2%). • PIRADS and PRI-MUS were strong predictors of CSPCa in a logistic regression model.	• No prior experience with micro-US. • Bias due to the lack of randomization and a control arm.
Abouassaly, 2020[117]	Single-center study	Micro-US	67	12-core SBx + 2- to 3-core mpMRI TBx + micro-US TBx	• Micro-US-guided targeting significantly increased the average grade group of cancer detected ($p < 0.01$) from conventional method.	• No prior experience with micro-US. • Single center with lack of blinding and randomization. • Inability to compare the value of micro-US and mpMRI due to the small sample size.
Grey, 2022[102]	Multicenter prospective paired-cohort study	mpUS (B-mode + CDUS + elastography + CEUS)	306	3-core mpUS TBx + 3-core mpMRI cognitive fusion TBx per lesion	• Positive test agreement between mpUS and mpMRI was 73.2% ($\kappa = 0.06$). • CSPCa detection by mpUS alone, mpMRI alone, and the combination of mpUS and mpMRI were 26%, 30%, and 32%, respectively. • 7% of CSPCa were exclusively detected by mpUS alone, whereas 20% of CSPCa were exclusively detected by mpMRI alone.	• mpMRI evaluation was based on the Likert system instead of PIRADS. • Each US imaging was evaluated with the standardized Likert scoring method, but the overall lesion score was at the discretion of the reporter.
Postema, 2020[96]	Multicenter prospective study	mpUS (B-mode + CEUS + CUDI)	133	RP histology	• Sensitivity, specificity, and AUC for CSPCa detection were 81%, 64%, and 0.78 for CEUS, 83%, 56%, 0.79 for CUDI, and 83%, 55%, and 0.78 for the combination, respectively. • Interobserver agreement for CEUS, CUDI, and the combination showed the weighted Fleiss Kappa values of 0.20, 0.18, and 0.18, respectively.	• Observers less trained to evaluate CEUS or CUDI. • Arbitrarily chosen Likert score. • RP histology as the reference standard potentially leads to selection bias.

(Continued)

Table 2. (Continued)

First author, year	Study design	Imaging modality	Number of patients	Reference standard	Main findings	Limitations
Wildeboer, 2020[97]	Single-center retrospective	mpUS (B-mode + SWE + CEUS)	48	RP histology	• mpUS classifier for CSPCa detection using random forest algorithm showed higher region-wise AUC than the best-performing single US radiomic parameter (0.90 *versus* 0.76). • Effective US radiomic features extracted from B-mode, elastography, and CEUS were not correlated with each other; therefore, may be cumulative.	• Single-center retrospective study design with small sample size. • RP histology as the reference standard potentially leads to selection bias.
Morris, 2020[98]	Retrospective study	mpUS (B-mode + ARFI + SWE + QUS)	35	RP histology	• mpUS evaluated with SVM method significantly outperformed B-mode and SWEI in PCa lesion visibility metrics (contrast, CNR and gCNR), and outperformed MF in contrast and CNR, and outperformed ARFI in CNR.	• Single-center retrospective study design with small sample size. • RP histology as the reference standard potentially leads to selection bias.
Drudi, 2019[99]	Prospective study	mpUS (B-mode + CDUS + CEUS + elastography)	82	MRI/US fusion 12 core SBx + 2 core TBx	• Sensitivity, specificity, and accuracy for PCa detection were 56.5%, 61.1%, and 58.5% for B-mode, 43.5%, 38.9%, and 41.5% for CDUS, and 40.0%, 97.2%, and 63.4% for quantitative analysis of CEUS, and 82.8%, 66.6%, and 76.8% for elastography, and 95.6%, 88.9%, and 92.7% for mpMRI, respectively.	• The performance of the combination of US modalities was not reported. • Suboptimal reference standard (no mpUS TBx).
Zhang, 2019[94]	Prospective comparative study between mpUS *versus* mpMRI	mpUS (B-mode + CDUS + SWE + CEUS)	78	12-core SBx	• Sensitivity, specificity, and AUC for localized PCa detection were 97.4%, 77.5%, and 0.87 for mpUS, 83%, 56%, 0.79 for CUDI, and 94.7%, 60% and 0.77 for the mpMRI, respectively.	• Suboptimal reference standard (no targeted PBx nor template PBx).
Mannaerts, 2019[95]	Single-center prospective study	mpUS (B-mode + SWE + CEUS)	48	RP histology	• mpUS showed 74% ROI-specific sensitivity and 59% specificity for CSPCa detection. • The sensitivity of mpUS was significantly higher in comparison with any single US modalities (B-mode, SWE, or CEUS). • The sensitivity of mpUS was higher for the PZ than the TZ (80% *versus* 67%). • Index lesion detection rate for mpUS was 88%, whereas those for B-mode, SWE, and CEUS were 72%, 70%, and 73%, respectively. • The Krippendorff α coefficient for mpUS was 0.33 for a Likert score $\geqslant$3 threshold and 0.46 for a Likert score $\geqslant$4 threshold.	• RP histology as the reference standard potentially leads to selection bias.

ANNA/C, computerized artificial neural network analysis; ARFI, acoustic radiation force impulse imaging; AUC, area under the curve; B-mode, brightness-mode; CDUS, color Doppler ultrasonography; CEUS, contrast-enhanced ultrasonography; CNR, contrast-to-noise ratio; CSPCa, clinically significant prostate cancer, CUDI, contrast ultrasound dispersion imaging; gCNR, generalized contrast-to-noise ratio; GG, grade group; GS, Gleason score; MCCL, maximum cancer core length; MF, midband fit; mpMRI, multiparametric magnetic resonance imaging; mpUS, multiparametric ultrasonography; MRI, magnetic resonance imaging; NPV, negative predictive value; OR, odds ratio; PBx, prostate biopsy; PCa, prostate cancer; PDUS, power Doppler ultrasonography; PHS, prostate HistoScanning; PIRADS, Prostate Imaging Reporting and Data System; PPV, positive predictive value; PRI-MUS, prostate risk identification using micro-ultrasound; PSA, prostate-specific antigen; PSAD, prostate-specific antigen density; PZ, peripheral zone; ROI, region of interest; RP, radical prostatectomy; SBx, systematic biopsy; SMI, superb microvascular imaging; STARD, standards for reporting diagnostic accuracy studies; SVM, support vector machine; SWE, shear-wave elastography; SWEI, shear wave elasticity imaging; TBx, targeted biopsy; TCCL, total cancer core length; TRUS, transrectal ultrasound; TT, true targeting; TTPM, template transperineal mapping; TZ, transitional zone; US, ultrasonography.

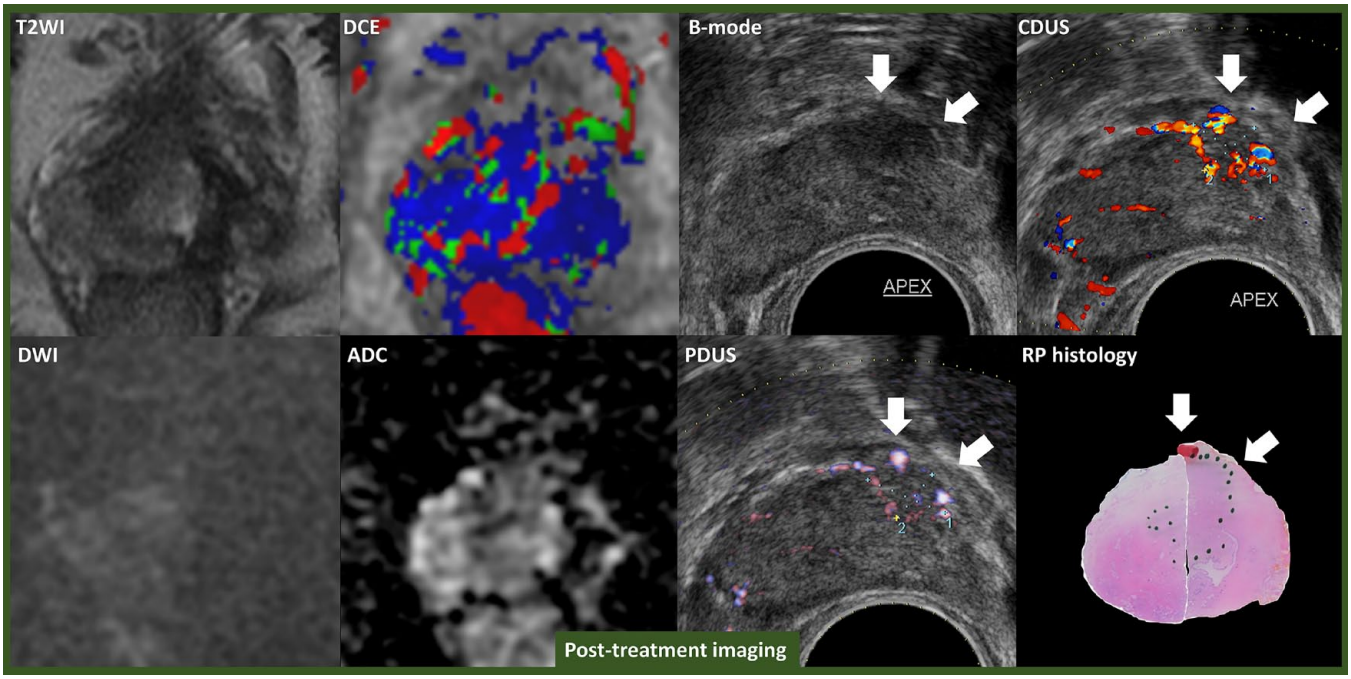

Figure 3. Representative images of negative on mpMRI but positive on mpUS. A 46-year-old man with PSA 7.0 ng/ml on active surveillance for GG1 cancer. Although surveillance mpMRI did not revealed PCa suspicious lesion, B-mode TRUS, CDUS, and PDUS detected 1.3 cm × 0.7 cm of PCa suspicious lesion on the left base of the prostate. Early enhancement was not observed on CEUS. Systematic biopsy + targeted biopsy to the PCa suspicious lesion detected GG2 PCa on the left base to mid area of the prostate. The patient selected left hemi-HIFU as a definitive treatment for PCa. Postoperatively, PSA dropped to 3.6 ng/ml, follow-up mpMRI did not show lesions suspicious for CSPCa (left figures). B-mode TRUS, CDUS, and PDUS detected 1 cm × 0.7 cm suspicious HEL on the left apex anterior area of the prostate (arrow on right figures), however. Targeted biopsy to the HEL revealed GG2 PCa recurrence. He underwent salvage robotic RP. GG2 PCa lesion with extraprostatic extension on the left anterior area was confirmed on RP histology specimen (green dots shows PCa mapping).
ADC, apparent diffusion coefficient; B-mode, brightness-mode; CDUS, color Doppler ultrasonography; CEUS, contrast-enhanced ultrasonography; CSPCa, clinically significant prostate cancer; DCE, dynamic contrast-enhanced imaging; DWI, diffusion-weighted imaging; GG, grade group; HEL, hypoechoic lesion; HIFU, high-intensity focused ultrasound; mpMRI, multiparametric magnetic resonance imaging; mpUS, multiparametric ultrasonography; PCa, prostate cancer; PDUS, power Doppler ultrasonography; PSA, prostate-specific antigen; RP, radical prostatectomy; T2WI, T2-weighted imaging; TRUS, transrectal ultrasound.

How to integrate multifactorial findings on each US modality can strongly affect the performance of mpUS; therefore, it is important to consider. Some investigators just added targeted biopsy to PCa suspicious lesion on any US modalities.[18,19] This strategy increases sensitivity and NPV, while it decreases specificity and PPV.[22] Other investigators scanned the prostate with strained elastography first to detect ROI, and they further screened whether the ROI is cancer suspicious on CEUS.[21] The strategy results in the increased specificity/PPV and the decreased sensitivity/NPV.[22] To optimize the performance of mpUS, some researchers used Likert-type scoring methods,[95,96,99] and others evaluated the existence of some imaging features.[94] Even when Likert-type scoring was performed, however, relatively low inter-reader agreement of mpUS was still a drawback.[95,96,118] It may be partly due to the nonstandardized mpUS reading process and the lack of well-validated and objective evaluation system. Currently, machine learning approach enables automated image recognition and providing quantitative assessments of massive number of complex radiographic characteristics.[119] Deep learning, a subset of machine learning, has already shown the equivalent diagnostic performance to that of health-care professionals.[120] To achieve more accurate and reproducible ultrasonographic assessments, as Wildeboer *et al.*[97] and Morris *et al.*[98] showed the feasibility in their studies, applying machine learning method on multifactorial radiomic features of mpUS is a promising approach.[119,121] Of note, as the complexity of machine learning algorithm increases, the developed model typically increases the performance but becomes less understandable algorithm. To overcome the limitation of machine learning method, the learning process should be interpretable by human, the number of radiomic features

to be evaluated should be minimum, and the biological interpretation/validation of the radiomic features are needed.[122] While 25% of CSPCa can be missed by mpMRI,[123] mpUS does detect CSPCa that was missed by mpMRI.[94] Integrated evaluation of both mpUS and mpMRI findings can be a fascinating future concept (Figure 3).

Conclusion

In the past 5 years, mpUS has exponentially gained popularity in urology and radiology field. Several latest evidence showed the potential of mpUS to provide more reliable performance for CSPCa detection and guidance for PBx and FT. Furthermore, some aspects including lower cost, real-time imaging, applicability for some patients who have contraindication for mpMRI, and availability in the office setting are clear strengths of mpUS. Machine learning approach and integration of radiomic features may improve the diagnostic performance of mpUS. Multicenter randomized controlled trials are warranted to directly compare the diagnostic performance of mpUS and mpMRI.

Declarations

Ethics approval and consent to participate

Not applicable.

Consent for publication

Written informed consent for publication were obtained from the patients.

Author contributions

Masatomo Kaneko: Conceptualization; Data curation; Formal analysis; Investigation; Methodology; Resources; Visualization; Writing – original draft; Writing – review & editing.

Maria Sarah L. Lenon: Data curation; Formal analysis; Investigation; Resources; Visualization; Writing – original draft; Writing – review & editing.

Lorenzo Storino Ramacciotti: Data curation; Formal analysis; Investigation; Writing – original draft; Writing – review & editing.

Luis G. Medina: Data curation; Formal analysis; Investigation; Writing – original draft; Writing – review & editing.

Aref S. Sayegh: Data curation; Formal analysis; Investigation; Writing – original draft; Writing – review & editing.

Anibal La Riva Rincon: Data curation; Formal analysis; Investigation; Writing – original draft; Writing – review & editing.

Laura C. Perez: Data curation; Formal analysis; Investigation; Writing – original draft; Writing – review & editing.

Alireza Ghoreifi: Data curation; Formal analysis; Investigation; Writing – original draft; Writing – review & editing

Maria Lizana: Data curation; Formal analysis; Investigation; Writing – original draft; Writing – review & editing.

Donya S. Jadvar: Writing – review & editing.

Amir H. Lebastchi: Conceptualization; Investigation; Methodology; Project administration; Supervision; Writing – review & editing.

Giovanni E. Cacciamani: Conceptualization; Investigation; Methodology; Project administration; Supervision; Writing – review & editing.

Andre Luis Abreu: Conceptualization; Data curation; Formal analysis; Investigation; Methodology; Project administration; Resources; Supervision; Visualization; Writing – review & editing.

Acknowledgements

None.

Funding

The authors received no financial support for the research, authorship, and/or publication of this article.

Competing interests

The authors declared the following potential conflicts of interest with respect to the research, authorship, and/or publication of this article: A.L.A. is the consulting physician for Koelis.

Availability of data and materials

Not applicable.

ORCID iDs

Masatomo Kaneko https://orcid.org/0000-0002-1205-807X
Aref S. Sayegh https://orcid.org/0000-0001-9320-2987
Anibal La Riva Rincon https://orcid.org/0000-0003-2198-833X
Maria Lizana https://orcid.org/0000-0002-0648-6043
Andre Luis Abreu https://orcid.org/0000-0002-9167-2587

References

1. Sung H, Ferlay J, Siegel RL, *et al*. Global cancer statistics 2020: GLOBOCAN estimates of incidence and mortality worldwide for 36 cancers in 185 countries. *CA Cancer J Clin* 2021; 71: 209–249.
2. Cooperberg MR, Lubeck DP, Meng MV, *et al*. The changing face of low-risk prostate cancer: trends in clinical presentation and primary management. *J Clin Oncol* 2004; 22: 2141–2149.
3. Smeenge M, Barentsz J, Cosgrove D, *et al*. Role of transrectal ultrasonography (TRUS) in focal therapy of prostate cancer: report from a consensus panel. *BJU Int* 2012; 110: 942–948.
4. Turkbey B, Pinto PA and Choyke PL. Imaging techniques for prostate cancer: implications for focal therapy. *Nat Rev Urol* 2009; 6: 191–203.
5. Stabile A, Giganti F, Rosenkrantz AB, *et al*. Multiparametric MRI for prostate cancer diagnosis: current status and future directions. *Nat Rev Urol* 2020; 17: 41–61.
6. Kaneko M, Sugano D, Lebastchi AH, *et al*. Techniques and outcomes of MRI-TRUS fusion prostate biopsy. *Curr Urol Rep* 2021; 22: 27.
7. Sugano D, Kaneko M, Yip W, *et al*. Comparative effectiveness of techniques in targeted prostate biopsy. *Cancers* 2021; 13: 1449.
8. Turkbey B, Rosenkrantz AB, Haider MA, *et al*. Prostate imaging reporting and data system version 2.1: 2019 update of prostate imaging reporting and data system version 2. *Eur Urol* 2019; 76: 340–351.
9. Das CJ, Razik A, Netaji A, *et al*. Prostate MRI–TRUS fusion biopsy: a review of the state of the art procedure. *Abdom Radiol* 2020; 45: 2176–2183.
10. Venderink W, de Rooij M, Sedelaar JPM, *et al*. Elastic versus rigid image registration in magnetic resonance imaging–transrectal ultrasound fusion prostate biopsy: a systematic review and meta-analysis. *Eur Urol Focus* 2018; 4: 219–227.
11. Hale GR, Czarniecki M, Cheng A, *et al*. Comparison of elastic and rigid registration during magnetic resonance imaging/ultrasound fusion-guided prostate biopsy: a multi-operator phantom study. *J Urol* 2018; 200: 1114–1121.
12. Ashi K, Kirkham B, Chauhan A, *et al*. Quantitative colour Doppler and greyscale ultrasound for evaluating prostate cancer. *Ultrasound* 2021; 29: 106–111.
13. Glybochko PV, Alyaev YG, Amosov AV, *et al*. Evaluation of prostate HistoScanning as a method for targeted biopsy in routine practice. *Eur Urol Focus* 2019; 5: 179–185.
14. Wildeboer RR, Postema AW, Demi L, *et al*. Multiparametric dynamic contrast-enhanced ultrasound imaging of prostate cancer. *Eur Radiol* 2017; 27: 3226–3234.
15. Correas JM, Tissier AM, Khairoune A, *et al*. Prostate cancer: diagnostic performance of real-time shear-wave elastography. *Radiology* 2015; 275: 280–289.
16. Lughezzani G, Saita A, Lazzeri M, *et al*. Comparison of the diagnostic accuracy of micro-ultrasound and magnetic resonance imaging/ultrasound fusion targeted biopsies for the diagnosis of clinically significant prostate cancer. *Eur Urol Oncol* 2019; 2: 329–332.
17. Dias AB, O'Brien C, Correas J-M, *et al*. Multiparametric ultrasound and micro-ultrasound in prostate cancer: a comprehensive review. *Br J Radiol* 2022; 95: 20210633.
18. Nelson ED, Slotoroff CB, Gomella LG, *et al*. Targeted biopsy of the prostate: the impact of color Doppler imaging and elastography on prostate cancer detection and Gleason score. *Urology* 2007; 70: 1136–1140.
19. Xie SW, Li HL, Du J, *et al*. Contrast-enhanced ultrasonography with contrast-tuned imaging technology for the detection of prostate cancer: comparison with conventional ultrasonography. *BJU Int* 2012; 109: 1620–1626.
20. Aigner F, Schäfer G, Steiner E, *et al*. Value of enhanced transrectal ultrasound targeted biopsy for prostate cancer diagnosis: a retrospective data analysis. *World J Urol* 2012; 30: 341–346.
21. Brock M, Eggert T, Palisaar RJ, *et al*. Multiparametric ultrasound of the prostate: adding contrast enhanced ultrasound to real-time elastography to detect histopathologically confirmed cancer. *J Urol* 2013; 189: 93–98.
22. Postema A, Mischi M, de la Rosette J, *et al*. Multiparametric ultrasound in the detection of prostate cancer: a systematic review. *World J Urol* 2015; 33: 1651–1659.
23. Grey A and Ahmed HU. Multiparametric ultrasound in the diagnosis of prostate cancer. *Curr Opin Urol* 2016; 26: 114–119.
24. Mottet N, Cornford P, van der Bergh R, *et al*. EAU-EANM-ESTRO-ESUR-SIOG guidelines on prostate cancer. European Association of Urology, 2022, https://d56bochluxqnz.cloudfront.net/documents/full-guideline/EAU-EANM-ESTRO-ESUR-ISUP_SIOG-Guidelines-on-Prostate-Cancer-2022_2022-04-25-063938_yfos.pdf (accessed 19 October 2022).

25. Azizi S, Mousavi P, Yan P, *et al*. Transfer learning from RF to B-mode temporal enhanced ultrasound features for prostate cancer detection. *Int J Comput Assist Radiol Surg* 2017; 12: 1111–1121.

26. Moradi M, Mousavi P and Abolmaesumi P. Computer-aided diagnosis of prostate cancer with emphasis on ultrasound-based approaches: a review. *Ultrasound Med Biol* 2007; 33: 1010–1028.

27. Porter CR and Wolff EM. *Prostate ultrasound volume 22*. New York, NY: Springer, 2015.

28. Meiburger KM, Acharya UR and Molinari F. Automated localization and segmentation techniques for B-mode ultrasound images: a review. *Comput Biol Med* 2018; 92: 210–235.

29. Postema AW, Scheltema MJV, Mannaerts CK, *et al*. The prostate cancer detection rates of CEUS-targeted versus MRI-targeted versus systematic TRUS-guided biopsies in biopsy-naïve men: a prospective, comparative clinical trial using the same patients. *BMC Urol* 2017; 17: 27.

30. Correas JM, Halpern EJ, Barr RG, *et al*. Advanced ultrasound in the diagnosis of prostate cancer. *World J Urol* 2021; 39: 661–676.

31. Steinkohl F, Luger AK, Pichler R, *et al*. Visibility of MRI prostate lesions on B-mode transrectal ultrasound. *Med Ultrason* 2018; 20: 441–445.

32. Chen FK, de Castro Abreu AL and Palmer SL. Utility of ultrasound in the diagnosis, treatment, and follow-up of prostate cancer: state of the art. *J Nucl Med* 2016; 57(Suppl. 3): 13S–18S.

33. Zhu YC, Shan J, Zhang Y, *et al*. Prostate cancer vascularity: Superb microvascular imaging ultrasonography with histopathology correlation. *Med Sci Monit* 2019; 25: 8571–8578.

34. Westendarp M, Postema A, de la Rosette JJ, *et al*. Advances in ultrasound techniques for the diagnosis and staging of prostate cancer. Elastography, Doppler ultrasound, ultrasound contrast media, ultrasound quantification media and MRI fusion. *Arch Esp Urol* 2015; 68: 307–315.

35. Kuligowska E, Barish MA, Fenlon HM, *et al*. Predictors of prostate carcinoma: accuracy of gray-scale and color Doppler US and serum markers. *Radiology* 2001; 220: 757–764.

36. Zeng S, Wu S, Chen C, *et al*. Performance characteristics of 3-D power Doppler ultrasound (3-D-PD) with the virtual organ computer-aided analysis (VOCAL) technique in the detection of prostate cancer. *Ultrasound Med Biol* 2022; 48: 91–97.

37. Sarıca Ö. Contribution of color Doppler sonography in the diagnosis of prostatic pathologies. *South Clin Istanbul Eurasia* 2019; 30: 255–260.

38. Ukimura O, de Castro Abreu AL, Gill IS, *et al*. Image visibility of cancer to enhance targeting precision and spatial mapping biopsy for focal therapy of prostate cancer. *BJU Int* 2013; 111: E354–E364.

39. Matsugasumi T, Iwata T, Yamada Y, *et al*. Intraoperative ultrasound monitoring with superb microvascular imaging in focal cryotherapy for prostate cancer. *J Med Ultrason* 2022; 49: 497–498.

40. Ohashi M, Shiraishi T, Fujihara A, *et al*. Detection of relatively poor but definitive blood supply in prostate stromal sarcoma using transrectal ultrasonography with superb microvascular imaging. *Int Cancer Conf J* 2022; 11: 215–218.

41. Boku H, Kaneko M, Yamada Y, *et al*. Microwave focal therapy of prostate cancer: a non-clinical study and exploratory clinical trial. *BJU Int*. Epub ahead of ahead of print 26 May 2022. DOI: 10.1111/bju.15749.

42. Morozov A, Kozlov V, Rivas JG, *et al*. A systematic review and meta-analysis of Histoscanning™ in prostate cancer diagnostics. *World J Urol* 2021; 39: 3733–3740.

43. Braeckman J, Autier P, Garbar C, *et al*. Computer-aided ultrasonography (HistoScanning): a novel technology for locating and characterizing prostate cancer. *BJU Int* 2008; 101: 293–298.

44. Wysock JS, Xu A, Orczyk C, *et al*. HistoScanning™ to detect and characterize prostate cancer – a review of existing literature. *Curr Urol Rep* 2017; 18: 97.

45. Scattoni V, Zlotta A, Montironi R, *et al*. Extended and saturation prostatic biopsy in the diagnosis and characterisation of prostate cancer: a critical analysis of the literature. *Eur Urol* 2007; 52: 1309–1322.

46. Simmons LAM, Kanthabalan A, Arya M, *et al*. Prostate imaging compared to transperineal ultrasound-guided biopsy for significant prostate cancer risk evaluation (PICTURE): a prospective cohort validating study assessing prostate HistoScanning. *Prostate Cancer Prostatic Dis* 2019; 22: 261–267.

47. Braeckman J, Autier P, Soviany C, *et al*. The accuracy of transrectal ultrasonography

supplemented with computer-aided ultrasonography for detecting small prostate cancers. *BJU Int* 2008; 102: 1560–1565.

48. Schiffmann J, Tennstedt P, Fischer J, *et al.* Does HistoScanning™ predict positive results in prostate biopsy? A retrospective analysis of 1,188 sextants of the prostate. *World J Urol* 2014; 32: 925–930.

49. Vezelis Alvydas A, Platkevicius G, Kincius KM, *et al.* Prostate 3D ultrasound-guided imaging device (HistoScanning) performance detecting clinically significant prostate cancer. *J BUON* 2020; 25: 460–463.

50. Macek P, Barret E, Sanchez-Salas R, *et al.* Prostate histoscanning in clinically localized biopsy proven prostate cancer: an accuracy study. *J Endourol* 2014; 28: 371–376.

51. Joyner CR Jr, Hey EB Jr, Johnson J, *et al.* Reflected ultrasound in the diagnosis of tricuspid stenosis. *Am J Cardiol* 1967; 19: 66–73.

52. de Castro Abreu AL, Ashrafi AN, Gill IS, *et al.* Contrast-enhanced transrectal ultrasound for follow-up after focal HIFU ablation for prostate cancer. *J Ultrasound Med* 2019; 38: 811–819.

53. Kundavaram CR, Halpern EJ and Trabulsi EJ. Value of contrast-enhanced ultrasonography in prostate cancer. *Curr Opin Urol* 2012; 22: 303–309.

54. Quaia E. Microbubble ultrasound contrast agents: an update. *Eur Radiol* 2007; 17: 1995–2008.

55. Brannigan M, Burns PN and Wilson SR. Blood flow patterns in focal liver lesions at microbubble-enhanced US. *Radiographics* 2004; 24: 921–935.

56. Porter TR, Mulvagh SL, Abdelmoneim SS, *et al.* Clinical applications of ultrasonic enhancing agents in echocardiography: 2018 American Society of Echocardiography guidelines update. *J Am Soc Echocardiogr* 2018; 31: 241–274.

57. Platts DG, Luis SA, Roper D, *et al.* The safety profile of perflutren microsphere contrast echocardiography during rest and stress imaging: results from an Australian multicentre cohort. *Heart Lung Circ* 2013; 22: 996–1002.

58. Seitz M, Gratzke C, Schlenker B, *et al.* Contrast-enhanced transrectal ultrasound (CE-TRUS) with cadence-contrast pulse sequence (CPS) technology for the identification of prostate cancer. *Urol Oncol* 2011; 29: 295–301.

59. Aigner F, Pallwein L, Mitterberger M, *et al.* Contrast-enhanced ultrasonography using cadence-contrast pulse sequencing technology for targeted biopsy of the prostate. *BJU Int* 2009; 103: 458–463.

60. Zhao HX, Xia CX, Yin HX, *et al.* The value and limitations of contrast-enhanced transrectal ultrasonography for the detection of prostate cancer. *Eur J Radiol* 2013; 82: e641–e647.

61. O'Neal D, Cohen T, Peterson C, *et al.* Contrast-enhanced ultrasound-guided radiofrequency ablation of renal tumors. *J Kidney Cancer VHL* 2018; 5: 7–14.

62. Guo S, Xu P, Zhou A, *et al.* Contrast-enhanced ultrasound differentiation between low- and high-grade bladder urothelial carcinomaand correlation with tumor microvessel density. *J Ultrasound Med* 2017; 36: 2287–2296.

63. Ashrafi AN, Nassiri N, Gill IS, *et al.* Contrast-enhanced transrectal ultrasound in focal therapy for prostate cancer. *Curr Urol Rep* 2018; 19:87.

64. Zhu Y, Chen Y, Jiang J, *et al.* Contrast-enhanced harmonic ultrasonography for the assessment of prostate cancer aggressiveness: a preliminary study. *Korean J Radiol* 2010; 11: 75–83.

65. Sano F and Uemura H. The utility and limitations of contrast-enhanced ultrasound for the diagnosis and treatment of prostate cancer. *Sensors* 2015; 15: 4947–4957.

66. Barr RG, Cosgrove D, Brock M, *et al.* WFUMB guidelines and recommendations on the clinical use of ultrasound elastography: part 5. *Ultrasound Med Biol* 2017; 43: 27–48.

67. Tsutsumi M, Miyagawa T, Matsumura T, *et al.* Real-time balloon inflation elastography for prostate cancer detection and initial evaluation of clinicopathologic analysis. *AJR Am J Roentgenol* 2010; 194: W471–W476.

68. Gennisson JL, Deffieux T, Fink M, *et al.* Ultrasound elastography: principles and techniques. *Diagn Interv Imaging* 2013; 94: 487–495.

69. Zhang B, Ma X, Zhan W, *et al.* Real-time elastography in the diagnosis of patients suspected of having prostate cancer: a meta-analysis. *Ultrasound Med Biol* 2014; 40: 1400–1407.

70. van Hove A, Savoie PH, Maurin C, *et al.* Comparison of image-guided targeted biopsies versus systematic randomized biopsies in the detection of prostate cancer: a systematic literature review of well-designed studies. *World J Urol* 2014; 32: 847–858.

71. Schiffmann J, Grindei M, Tian Z, *et al.* Limitations of elastography based prostate biopsy. *J Urol* 2016; 195: 1731–1736.

72. Anbarasan T, Wei C, Bamber JC, *et al*. Characterisation of prostate lesions using transrectal shear wave elastography (SWE) ultrasound imaging: a systematic review. *Cancers* 2021; 13: 1–15.

73. Fu S, Tang Y, Tan S, *et al*. Diagnostic value of transrectal shear wave elastography for prostate cancer detection in peripheral zone: comparison with magnetic resonance imaging. *J Endourol* 2020; 34: 558–566.

74. Xiang LH, Fang Y, Wan J, *et al*. Shear-wave elastography: role in clinically significant prostate cancer with false-negative magnetic resonance imaging. *Eur Radiol* 2019; 29: 6682–6689.

75. Miyagawa T, Tsutsumi M, Matsumura T, *et al*. Real-time elastography for the diagnosis of prostate cancer: evaluation of elastographic moving images. *Jpn J Clin Oncol* 2009; 39: 394–398.

76. Kanagaraju V, Ashlyin PVK, Elango N, *et al*. Role of transrectal ultrasound elastography in the diagnosis of prostate carcinoma. *J Med Ultrasound* 2020; 28: 173–178.

77. Correas JM, Tissier AM, Khairoune A, *et al*. Ultrasound elastography of the prostate: state of the art. *Diagn Interv Imaging* 2013; 94: 551–560.

78. Pavlovich CP, Cornish TC, Mullins JK, *et al*. High-resolution transrectal ultrasound: pilot study of a novel technique for imaging clinically localized prostate cancer. *Urol Oncol* 2014; 32: 34.e27–34.e32.

79. Harland N and Stenzl A. Micro-ultrasound: a way to bring imaging for prostate cancer back to urology. *Prostate Int* 2021; 9: 61–65.

80. McNeal JE. Normal histology of the prostate. *Am J Surg Pathol* 1988; 12: 619–633.

81. Ghai S, Eure G, Fradet V, *et al*. Assessing cancer risk on novel 29 MHz micro-ultrasound images of the prostate: creation of the micro-ultrasound protocol for prostate risk identification. *J Urol* 2016; 196: 562–569.

82. Feleppa EJ. Basic physics of diagnostic ultrasound. In: Porter CR and Wolff EM (eds) *Prostate ultrasound*. New York: Springer, 2015, pp. 31–56.

83. Terris MK and Stamey TA. Determination of prostate volume by transrectal ultrasound. *J Urol* 1991; 145: 984–987.

84. Claros OR, Tourinho-Barbosa RR, Fregeville A, *et al*. Comparison of initial experience with transrectal magnetic resonance imaging cognitive guided micro-ultrasound biopsies versus established transperineal robotic ultrasound magnetic resonance imaging fusion biopsies for prostate cancer. *J Urol* 2020; 203: 918–925.

85. Eure G, Fanney D, Lin J, *et al*. Comparison of conventional transrectal ultrasound, magnetic resonance imaging, and micro-ultrasound for visualizing prostate cancer in an active surveillance population: a feasibility study. *Can Urol Assoc J* 2019; 13: E70–E77.

86. Pavlovich CP, Hyndman ME, Eure G, *et al*. A multi-institutional randomized controlled trial comparing first-generation transrectal high-resolution micro-ultrasound with conventional frequency transrectal ultrasound for prostate biopsy. *BJUI Compass* 2021; 2: 126–133.

87. Cornud F, Lefevre A, Flam T, *et al*. MRI-directed high-frequency (29 MHz) TRUS-guided biopsies: initial results of a single-center study. *Eur Radiol* 2020; 30: 4838–4846.

88. Wiemer L, Hollenbach M, Heckmann R, *et al*. Evolution of targeted prostate biopsy by adding micro-ultrasound to the magnetic resonance imaging pathway. *Eur Urol Focus* 2021; 7: 1292–1299.

89. Zhang M, Wang R, Wu Y, *et al*. Micro-ultrasound imaging for accuracy of diagnosis in clinically significant prostate cancer: a meta-analysis. *Front Oncol* 2019; 9: 1368–1369.

90. Sountoulides P, Pyrgidis N, Polyzos SA, *et al*. Micro-ultrasound-guided vs multiparametric magnetic resonance imaging-targeted biopsy in the detection of prostate cancer: a systematic review and meta-analysis. *J Urol* 2021; 205: 1254–1262.

91. Dariane C, Ploussard G, Barret E, *et al*. Micro-ultrasound-guided biopsies versus systematic biopsies in the detection of prostate cancer: a systematic review and meta-analysis. *World J Urol*. Epub ahead of print 14 July 2022. DOI: 10.1007/s00345-022-04087-z.

92. Klotz L, Lughezzani G, Maffei D, *et al*. Comparison of micro-ultrasound and multiparametric magnetic resonance imaging for prostate cancer: a multicenter, prospective analysis. *Can Urol Assoc J* 2020; 15: E11–E16.

93. Klotz L, Andriole G, Cash H, *et al*. Optimization of prostate biopsy – micro-ultrasound versus MRI (OPTIMUM): a 3-arm randomized controlled trial evaluating the role of 29 MHz micro-ultrasound in guiding prostate biopsy in men with clinical suspicion of prostate cancer. *Contemp Clin Trials* 2022; 112: 106618.

94. Zhang M, Tang J, Luo Y, *et al*. Diagnostic performance of multiparametric transrectal

ultrasound in localized prostate cancer: a comparative study with magnetic resonance imaging. *J Ultrasound Med* 2019; 38: 1823–1830.

95. Mannaerts CK, Wildeboer RR, Remmers S, *et al*. Multiparametric ultrasound for prostate cancer detection and localization: correlation of B-mode, shear wave elastography and contrast enhanced ultrasound with radical prostatectomy specimens. *J Urol* 2019; 202: 1166–1173.
96. Postema AW, Gayet MCW, van Sloun RJG, *et al*. Contrast-enhanced ultrasound with dispersion analysis for the localization of prostate cancer: correlation with radical prostatectomy specimens. *World J Urol* 2020; 38: 2811–2818.
97. Wildeboer RR, Mannaerts CK, van Sloun RJG, *et al*. Automated multiparametric localization of prostate cancer based on B-mode, shear-wave elastography, and contrast-enhanced ultrasound radiomics. *Eur Radiol* 2020; 30: 806–815.
98. Morris DC, Chan DY, Lye TH, *et al*. Multiparametric ultrasound for targeting prostate cancer: combining ARFI, SWEI, QUS and B-Mode. *Ultrasound Med Biol* 2020; 46: 3426–3439.
99. Drudi FM, Cantisani V, Angelini F, *et al*. Multiparametric MRI versus multiparametric US in the detection of prostate cancer. *Anticancer Res* 2019; 39: 3101–3110.
100. Pepe P, Pepe L, Panella P, *et al*. Can multiparametric ultrasound improve cognitive MRI/TRUS fusion prostate biopsy. *Arch Ital Di Urol E Androl* 2020; 92: 89–92.
101. Fanti S, Minozzi S, Antoch G, *et al*. Consensus on molecular imaging and theranostics in prostate cancer. *Lancet Oncol* 2018; 19: e696–e708.
102. Grey ADR, Scott R, Shah B, *et al*. Multiparametric ultrasound versus multiparametric MRI to diagnose prostate cancer (CADMUS): a prospective, multicentre, paired-cohort, confirmatory study. *Lancet Oncol* 2022; 23: 428–438.
103. Shaeffer EM, Sriniva S, An Y, *et al*. NCCN guideline prostate cancer version 1.2023, https://www.nccn.org/professionals/physician_gls/pdf/prostate.pdf (accessed 19 October 2022).
104. Mehralivand S, Shih JH, Rais-Bahrami S, *et al*. A magnetic resonance imaging–based prediction model for prostate biopsy risk stratification. *JAMA Oncol* 2018; 4: 678–685.
105. Lorusso V, Kabre B, Pignot G, *et al*. External validation of the computerized analysis of TRUS of the prostate with the ANNA/C-TRUS system: a potential role of artificial intelligence for improving prostate cancer detection. *World J Urol*. Epub ahead of print 6 March 2022. DOI: 10.1007/s00345-022-03965-w.
106. Garcia-Reyes K, Nguyen HG, Zagoria RJ, *et al*. Impact of lesion visibility on transrectal ultrasound on the prediction of clinically significant prostate cancer (Gleason score 3 + 4 or greater) with transrectal ultrasound-magnetic resonance imaging fusion biopsy. *J Urol* 2018; 199: 699–705.
107. Sharen GW and Zhang J. Application of shear wave elastography and contrast-enhanced ultrasound in transrectal prostate biopsy. *Curr Med Sci* 2022; 42: 447–452.
108. Baur ADJ, Schwabe J, Rogasch J, *et al*. A direct comparison of contrast-enhanced ultrasound and dynamic contrast-enhanced magnetic resonance imaging for prostate cancer detection and prediction of aggressiveness. *Eur Radiol* 2018; 28: 1949–1960.
109. Eldred-Evans D, Burak P, Connor MJ, *et al*. Population-based prostate cancer screening with magnetic resonance imaging or ultrasonography: the IP1-PROSTAGRAM study. *JAMA Oncol* 2021; 7: 395–402.
110. Liang L, Zhi X, Sun Y, *et al*. A nomogram based on a multiparametric ultrasound radiomics model for discrimination between malignant and benign prostate lesions. *Front Oncol* 2021; 11: 610785–610712.
111. Ji Y, Ruan L, Ren W, *et al*. Stiffness of prostate gland measured by transrectal real-time shear wave elastography for detection of prostate cancer: a feasibility study. *Br J Radiol* 2019; 92: 20180970.
112. Ding Z, Jiao Y, Wu H, *et al*. Clinical value of the elastographic Q-analysis score in assisting real-time elastography-guided prostate Biopsy: a retrospective study of 125 patients. *J Ultrasound Med* 2020; 39: 83–87.
113. Lughezzani G, Maffei D, Saita A, *et al*. Diagnostic accuracy of microultrasound in patients with a suspicion of prostate cancer at magnetic resonance imaging: a single-institutional prospective study. *Eur Urol Focus* 2021; 7: 1019–1026.
114. Chessa F, Schiavina R, Amelio E, *et al*. Diagnostic accuracy of the novel 29 MHz micro-ultrasound 'ExactVuTM' for the detection of clinically significant prostate cancer: a prospective single institutional study. A step forward in the diagnosis of prostate cancer. *Arch Ital Di Urol E Androl* 2021; 93: 132–138.

115. Avolio PP, Lughezzani G, Paciotti M, *et al*. The use of 29 MHz transrectal micro-ultrasound to stratify the prostate cancer risk in patients with PI-RADS III lesions at multiparametric MRI: a single institutional analysis. *Urol Oncol* 2021; 39: 832e1–832.e7.

116. Rodríguez Socarrás ME, Gomez Rivas J, Cuadros Rivera V, *et al*. Prostate mapping for cancer diagnosis: the Madrid protocol. Transperineal prostate biopsies using multiparametric magnetic resonance imaging fusion and micro-ultrasound guided biopsies. *J Urol* 2020; 204: 726–733.

117. Abouassaly R, Klein EA, El-Shefai A, *et al*. Impact of using 29 MHz high-resolution micro-ultrasound in real-time targeting of transrectal prostate biopsies: initial experience. *World J Urol* 2020; 38: 1201–1206.

118. Park KJ, Choi SH, Lee JS, *et al*. Interreader agreement with prostate imaging reporting and data system version 2 for prostate cancer detection: a systematic review and meta-analysis. *J Urol* 2020; 204: 661–670.

119. Hosny A, Parmar C, Quackenbush J, *et al*. Artificial intelligence in radiology. *Nat Rev Cancer* 2018; 18: 500–510.

120. Liu X, Faes L, Kale AU, *et al*. A comparison of deep learning performance against health-care professionals in detecting diseases from medical imaging: a systematic review and meta-analysis. *Lancet Digit Health* 2019; 1: e271–e297.

121. Sugano D, Sanford D, Abreu A, *et al*. Impact of radiomics on prostate cancer detection: a systematic review of clinical applications. *Curr Opin Urol* 2020; 30: 754–781.

122. Castiglioni I, Rundo L, Codari M, *et al*. AI applications to medical images: from machine learning to deep learning. *Phys Med* 2021; 83: 9–24.

123. Ahmed HU, El-Shater Bosaily A, Brown LC, *et al*. Diagnostic accuracy of multi-parametric MRI and TRUS biopsy in prostate cancer (PROMIS): a paired validating confirmatory study. *Lancet* 2017; 389: 815–822.